Master's Thesis

Numerical analysis of neuronal responses for photolysis of MNI and Rubi caged glutamate

Jeonghyeon Lee

Department of Biomedical Engineering

Graduate School of UNIST

2017

Numerical analysis of neuronal responses for photolysis of MNI and Rubi caged glutamate

Jeonghyeon Lee

Department of Biomedical Engineering

Graduate School of UNIST

Numerical analysis of neuronal responses for photolysis of MNI and Rubi caged glutamate

A thesis/dissertation
submitted to the Graduate School of UNIST
in partial fulfillment of the
requirements for the degree of
Master of Science

Jeonghyeon Lee

1. 20. 2017

Approved by

Advisor
Woonggyu Jung

Numerical analysis of neuronal responses for photolysis of MNI and Rubi caged glutamate

Jeonghyeon Lee

This certifies that the thesis/dissertation of Jeonghyeon Lee is approved.

1. 20. 2017

signature

Advisor: Woonggyu Jung

signature

typed name: Cheol-Min Ghim

signature

typed name: Hyung Joon Cho

Abstract

Photo-labile caged compound are biologically inert state, but absorption of flash light unleash the cleavage of chemical bond so that bioactive molecules come out and have influence on cellular dynamics in various ways. Such uncaging method with advanced optical technique is possible to manipulate the function of cell with high subcellular resolution. However, there have been no suitable quantification method of the amount of photolysis in situ. Fluorescence indicators have not been made for caged compounds with the exception of specific bioactive molecules such as peptide and $Ca2^{+}$.

In this paper, we investigated evoked neuronal responses for photolysis of MNI and Rubi-caged glutamate, and suggested a new formula quantifying the extent of the uncaging. For those, primary hippocampal neurons were cultured on Microelectrode-array (MEA) with microfluidic devices for recording extracellular signals. Evoked neuronal responses was monitored according to optical stimulation parameters including wavelength, intensity, illumination duration and concentration of each chemicals respectively. Our experimental results revealed that the number of spikes per second was dependent on illumination power, wavelength, exposure time and concentration. Also, the first neural response was involved in illuminated intensity of light regardless of chemical species of caged glutamate. Those result indicated that three optical factors and concentration, were important factors to determine the amount of released glutamates. Finally, we established a new formula quantifying the amount of released glutamate. Through an empirical assessment, neuronal responses could be elicited by numerically modeling the amount of the released caged glutamates. We hoped that this formula was applied in quantification of the amount of photolysis of various caged compounds.

Keyword: Caged glutamate, Optical stimulation, Microelectrode-array (MEA), Neural recording

Contents

List of Figures

List of Tables

List of Formula

Chapter 1. Introduction.

Caged compounds are light-sensitive organic molecules that protect functionally bioactive molecules, chemically attached by a protecting group or caging group. A molecule of interest was synthesized with photo-removable protecting group and maintained biologically inactive. A flash light caused bond cleavage of it generating biologically active molecule. The initial strategies appeared in the late 1970s **[1, 2]**. Since then, various signaling molecule or second messenger, including even small proteins and nucleic acids, was chemically synthesized (or caged) for cellular biology, physiology and neuroscience **[3]**. Representative caged compounds or second messengers are AMP **[1]**, ATP **[2]**, calcium **[4-7]**, inositols **[8]**, peptides **[9]**, enzymes **[10]**, carbamoylcholine **[11]**, mRNA **[12]** and DNA **[13]**. And as last phase, caged neurotransmitters started to be developed including glutamate, GABA, serotonin and glycine **[14-22]**. And many cage glutamate molecules was commercially available as shown in **Table. 1-1 [23]**.

Recent researches pursued the development of photo-protective group with high photochemical efficiencies for near-UV and visible absorption **[24]**. Because absorption of wavelength UV light oxygen and nitrogen species, which could ruin DNA and membrane lipid **[25]**. Also, longer wavelength have advantage of two-photon excitation in penetration depth **[24]**.

Caged Glu.	ε (λmax)	Φ (% Glu yield)	ε·Φ	Commercial	Stability in aqueous buffer	Solubility (mM) at pH 7.4 In aqueous Buffer
Noc	500 (350)	0.65 (100)	325	none	Stable	>50
CNB	500(350)	0.14(100)	60	Invitrogen	Half-life 17 h rt	>50
MNI	4,300(330)	0.085 (>95)	357	Tocris	Stable	400
RuBi	5,600 (450)	0.13 (NQ)	728	Tocris	Stable	NR
PMNB	9,900 (317)	0.1 (100)	990	none	Stable	Requires 1% DMSO
antMNI	27,000 (300)	0.085 (94)	2295	none	Stable	33
BNSF	64,000 (415)	0.25 (65)	16,000	none	ND	0.1
CDNI	6,400 (330)	0.6 (100)	3,840	none	Stable pH 2	100
DEAC	13,700 (390)	0.11 (NQ)	1507	none	stable	NR
MANI	4,300 (330)	0.1 (100)	430	Sigma	Like MNI	>100
Bhc	43,000 (458)	0.3 (100)	12,900	none	Stable frozen pH 7.4	7.5

Table 1-1. Properties of various caged glutamate probe [23]. Abbreviations and symbols: ε, extinction coefficient; Φ, quantum yield;

With the development of synthetic organic chemistry, optical technique for photolysis of caged compounds have been studied in illuminating system, including scanning laser photo-stimulation in single and two-photon, holographic illumination and fiber-optic lightguides. Optical stimulation of photolysis acted as functional synaptic input and was applied in mapping of glutamic receptor **[**26**]**. Dalva et al 1994, discovered the declines in local connections on the activity of layer 2 and layer 3 neurons in visual cortex with scanning laser photo-stimulation **[27]**. And mapping NMDA and AMPA receptor revealed differentially distribution of both receptors on dendrites **[28]**, and hot spots on apical dendrite **[29]**. Also, it was contributed to discover that Long-term depression (LTD) was dependent on NMDA-receptor **[30]** and varied with the distance **[31]**. Also, glutamate uncaging method demonstrated the relation transient calcium influx to active NMDA receptor **[30]**, and regulation of subunit composition of their NMDA-R and Ca^{2+} currents **[32]**. Yang et al reported specific patterns of $Ca2^{+}$ elevation as long as LTP or LTD with caged calcium compound **[33]**.

As a one of areas in adaptive optics, holographic illumination for photolysis of caged compounds was applied in complex photo-activation patterns **[34-41]**. Basically, it could modulate the distribution and shape of light using spatial light modulator (SLM). Consequently, such beam-shaping techniques can control multiple spots of variable size and number, and shape illumination for two or three dimensional photo-stimulation. These techniques have been studied for holographic photolysis of caged compounds with shaped illumination in single-photon **[35, 36]** and two-photon **[37, 38]** in a single plane, and for a 3D multi-foci photo-stimulation pattern in single-photon **[39,40]** and two-photon **[34, 41]**. This promising methods allowed us to mimic complex, simultaneous synaptic inputs with sub millisecond speed in three-dimension. As other solution, a fiber optic was introduced to expand the field of caged compounds for *in vitro* and *in vivo* experiment **[42-44, 45]**. Especially, tapered fiber-optic light guides could adjust the effective volume of uncaging by controlling the end of fiber **[42, 43]**.

Quantification of the released amount of photolysis have significantly importance on analysis in the molecular biology and neuroscience. Because small fluctuation of bioactive molecules could have a catastrophic effect in the cellular response and it's regulating system such as excitotoxicity **[46]**. Previous studies depended on increase of fluorescence intensity resulting from the released of caged compounds for a quantitative analysis of the uncaging reaction. However, it is limited to specific molecules in the massive molecules such as peptides or proteins **[47]**, or $Ca2^{+}$ with well-developed fluorescent indicators **[48, 49]**. In most case, suitable probes have not been invented for other caged compounds **[50]**. In case of glutamate, conventional methods for glutamate concentration was determined by microdialysis. However, it is invasive sampling technique by poor spatial and temporal resolution. Recent intensity-based glutamate-sensing fluorescent reporter (iGluSnFR) was developed by bacterial periplasmic binding proteins, inserting circularly permuted fluorescent proteins with SNR and kinetics **[51]**.

Here, we studied photochemical properties of MNI and Rubi-caged glutamate in cultured hippocampal neuron on MEA combined with microfluidic chips. In order to comprehend photochemical properties (extinction coefficient and quantum yield) of both chemicals, various optical stimulation condition is applied in experiments. Optically evoked activities were recorded by MEA and analyzed with spike-sorting technique. Firstly, it is verified that response of photolysis correspond approximately to glutamatergic activities by comparison of waveforms in both. Also, the number of evoked spikes per sec was dependent on wavelength, illuminating power, exposure duration and concentration of caged compounds. Higher illuminating power, exposure duration and concentration evoked more spikes per sec. In contrast, the number of spikes was followed by absorption of each chemicals. Furthermore, the first response time from onset was in inverse proportion to illuminating power. Those results indicated that three optical factors and concentration determined the amount of released glutamates. Finally, we could quantify the uncaging with the known photochemical characteristic suggesting a new established equation. Numerical modeling of estimated amount of uncaged glutamate had similar tendency to experiment data. Our research could contribute to quantification of the amount of various uncaged bioactive molecules.

1. 1. Overview

1.1.1 Overview of glutamatergic excitation

L-glutamate is the most important excitatory neurotransmitter in the nervous system **[52]**, as its release at the synapses deliver electrical signals chemically from presynaptic to postsynaptic neurons. So, excitatory chemical synapses evoke an excitatory postsynaptic potential (EPSP) on the postsynaptic neurons. Furthermore, glutamate is linked to many other cellular signaling. And also glutamate receptors, which bind released glutamate, are found throughout the nerve system in neurons and astrocytes **[23]**.

Photolysis of caged glutamate as one of photo-stimulation techniques mimics synaptic activation by photo-release of L-glutamate. To enhance the comprehension of our experiment, the following overview will describe glutamate receptor and the mechanisms of glutamatergic excitation in the nerve synapses briefly.

Glutamate receptors

As the major excitatory receptor, glutamate receptors (GluRs) divide into two categories, ionotropic (voltage sensitive) and metabotropic (ligand sensitive) **[52]**. Ionotropic GluRs can be subdivided into three main types according to their sensitivity to alpha-amino-3-hydroxy-5-methyl-4-isoxazolepropionic acid (AMPA), Kainate, and N-Methyl-D-aspartic acid (NMDA).

Glutamatergic excitation

Action potential in the presynaptic neuron induces the release of glutamate from the presynaptic terminals. The released glutamate binds to glutamate receptor located at the postsynaptic membrane. AMPA and kainite receptors permit conduction of sodium ions, which depolarize EPSP of the postsynaptic cell. The depolarization through the above receptors initiate the relief of magnesium ions that block NMDA receptors, and NMDA-receptor mediate a calcium ions in the extracellular environment. Finally, calcium, which is a central messenger molecule, activate second-messenger signaling pathways in the postsynaptic cell, retaining persistent activation of two protein kinases and taking in glutamate actively on the postsynaptic neuron. In summary, **Fig. 1-1** explain the mechanisms of glutamatergic synapses in the axon terminals.

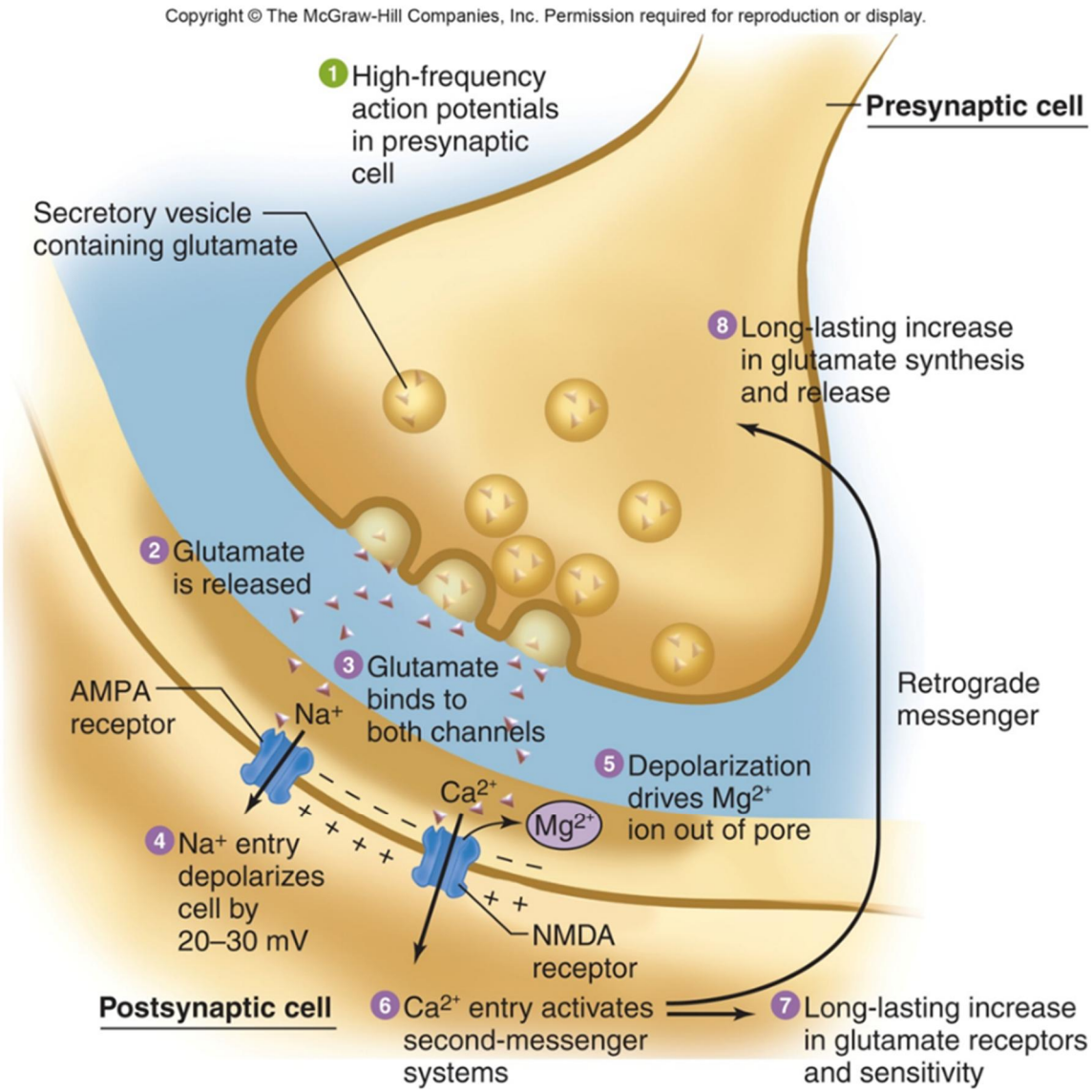

Figure 1-1. The mechanisms of glutamatergic synapses in the axon terminals [53]

1.1.2 Characterization of photochemical uncaging efficiency by photolysis of one-photon stimulation

The uncaging efficiency of one-photon photolytic reaction at a given wavelength is normally defined in terms of the product ($\varepsilon \times \Phi$) of extinction coefficient (ε in $M^{-1}cm^{-1}$) and quantum yield (Φ in Extinction coefficient is derived from light absorption, which is quantified parameter how strongly a subject absorbs light depending on a given wavelength. So if a certain subject has large extinction coefficient or light absorption, it is likely to absorb a photon. Absorption (A) can be measured by spectrophotometer based on Beers-Bougert-Lambert law as shown below. And finally we can calculate extinction coefficient with the already known concentration of solution and the physical length of cuvette.

$$A = -\log T = -\log \frac{I}{I_o} = \log \frac{I_o}{I} = \varepsilon dc,\ \varepsilon = \frac{A}{dc}$$

Where T = transmission, I_0 = the intensity of incident intensity, I = the intensity of transmitted intensity, d =physical path length (cm), c = concentration (M)

$$\Phi\ (\text{moles per Einstein or } \frac{\text{number of moles converted}}{\text{number of quanta absorbed}})$$

The quantum yield (Φ) of one-photon photolytic reaction is defined as how many excited state molecules are converted into uncaged glutamate **[50]**. There are mainly two methods to determine quantum yield of one-photon photolytic reaction: (1) direct measurement method and (2) indirect comparison method **[54]**. In regard to direct measurement method, the quantum yield is derived from measurements of photon flux and rate of reaction. The photon flux Ep for irradiated caged glutamate solution at specific wavelength can be measured by chemical actinometry **[54].**

$$Ep = 5.30 \times 10^{-6}\ \Delta A_{wave}/\Delta t[Einstein\ cm^{-2}s^{-1}]$$

$\Delta A_{wave} = the\ value\ of\ change\ in\ absorbance\ at\ specific\ wavelength$
$\Delta t = the\ irradiation\ time\ in\ second$

In the while, rate of reaction is defined as change in the uncaging concertation of the compound versus time (in second) induced by irradiation of monochromatic light **[54]**. Analytic method like High Performance Liquid Chromatography (HPLC) can observe the reaction progress. Finally, the quantum yield (Φ) of one-photon photolytic reaction is calculated by the above equation by using two acquisitions of photon flux and rate **[54]**.

$$\Phi = \frac{\Delta c}{\Delta t} \times Ep^{-1} \times V$$

$$V = the\ volume\ of\ the\ irradated\ solution$$

The quantum yield of one-photon photolytic reaction can be measured easily as indirect comparison method with a caged compound, which have already known quantum yield **[54]**.

$$\Phi_u = \Phi_u\ (\text{reference}) \times \text{Grad[Sustance]/Grad[Reference]}$$

Where Grad [Reference] = rate of reaction about reference, Grad [substance] = rate of reaction about 1:1 mixture of reference and unknown caged compound, Φu= quantum yield for reference.

Chapter 2. Experimental Methods and Equipments

2.1 Experimental set-up

The experiment set-up was built around an inverted microscope (IX70 Olympus, Japan) including a customized culture chamber (Live cell instruments, Korea), A CCD camera (Hamamatsu, Japan), the MEA 1060-inv-BC system (Multichannel Systems, Germany) and LED light source, as shown in **Fig. 2-1**. A continuous UV-visible light from SOLA light engine [Lumencor, USA, **Fig. 2-6-(b)**] enters the microscope and reaches the back aperture of an objective lens. By passing through 0.7 N.A 60x objective lens (Olympus, Japan) and 1 mm thick glass microelectrode arrays, it is illuminated to cultured neurons.

The experiment set-up is equipped with customized chamber (Live cell instruments, Korea), 37^{o}C temperature controller and a humidified 5% CO_2 gas inlet in order to enhance viability and stabilization of cultured neurons. Established microscopic set-up with CCD camera helps to observe the position of electrode and targeted cell instantly. Also, two installed motorized stage, XY-auto stage (Live Cell instruments, Korea) and Z-motorized stage (Applied Scientific Instruments, USA), can facilitate the fine adjustment of focused light spatially.

The microfluidic device was fabricated with the replica molding of the PDMS (Polydimethylsiloxane). For preparation of replica molding, process of photolithography including treatment for wafer and micro-patterned mask was explained more detail in our previous study **[55].** Microfluidic device was designed to separate physically the axons in a micro-groove from the soma in a micro-channel [**Fig. 2-1-(c)**]. Fabricated PDMS are attached on MEA after rinsing with distilled water three times. It was treated with oxygen plasma for 4 minutes 30 seconds to make the surface hydrophilic. Before cell plating, Poly-D-lysine (PDL) coating in 2 hour promotes the adhesion of cells to the surface of MEA

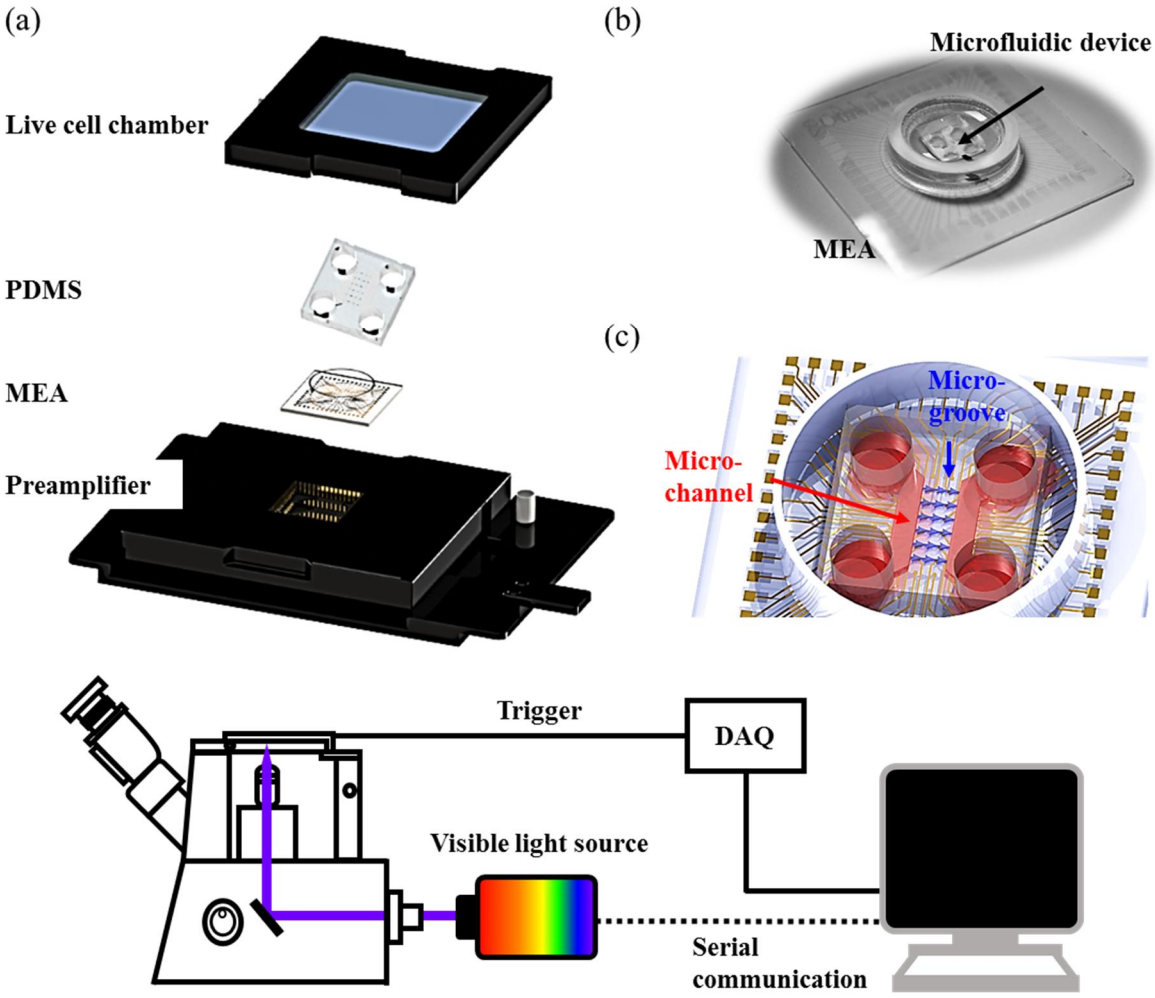

Figure 2-1. Scheme of the developed set-up.

(a) UV-visible light for photolysis of caged glutamate was delivered into cultured neurons in the microfluidic culture chip. Each time neurons in the live cell chamber are photo-stimulated, neural responses from 60-channels were recorded simultaneously. Actual image (b) and a diagram (c) of a microfluidic device embedded in microelectrode array.

2.2 Primary cell culture

Material

Hank's Balenced Salt Sodium (HBSS) (Gibco, USA)

B27 supplement (Gibco, USA)

Neurobasal Medium (Gibco, USA)

Sprague-Dawley rats (Hyochang Science, Korea)

Trypsin-EDTA (Gibco, USA)

GlutaMAX™ Supplement (Gibco, USA)

Primocin (InvivoGen, USA)

Poly-D-lysine (PDL) (Sigma, USA)

Micro forceps and micro scissor

All animal procedures were performed in accordance with the guidelines of the Ulsan National Institute of Science and Technologies Institutional Animal Care and use Committee. After a high level of carbon dioxide (CO_2) anesthesia, primary hippocampal neurons were isolated from embryonic day 17 ~ 18 (E17-E18) rats, bred from pregnant Sprague-Dawley rats. The rat brains were removed from the embryos and their hippocampal neurons were rapidly dissected from cortex at 4 °C in HBSS. After being dissociated in 0.25 % trypsin–EDTA solution for 15 min in a water bath at 37 °C, DMEM containing 10% horse serum was added into solution to stop the trypsinization. After the supernatant were removed, the cell was transferred into culture media containing neurobasal media supplemented with B27 (20 mL/L), GlutaMax (2.5 mL/L) and Primocin (100 μg/ml). And the cell were plated at a concentration of $3 \sim 6 \times 10^6$ cell per mL in a MEA surface coated with PDL. The neurons were incubated at 37 °C in air containing 5 % CO_2 for 7 ~ 14 days before experiment. Neurons with the fluorescently labeled Tau protein (Green) and DAPI (blue) were observed on Multi-Photon Confocal Microscopy LSM 780NLO (Zeiss, Japan) in UNIST Optical Biomed Imaging Center (**Fig. 2-2**).

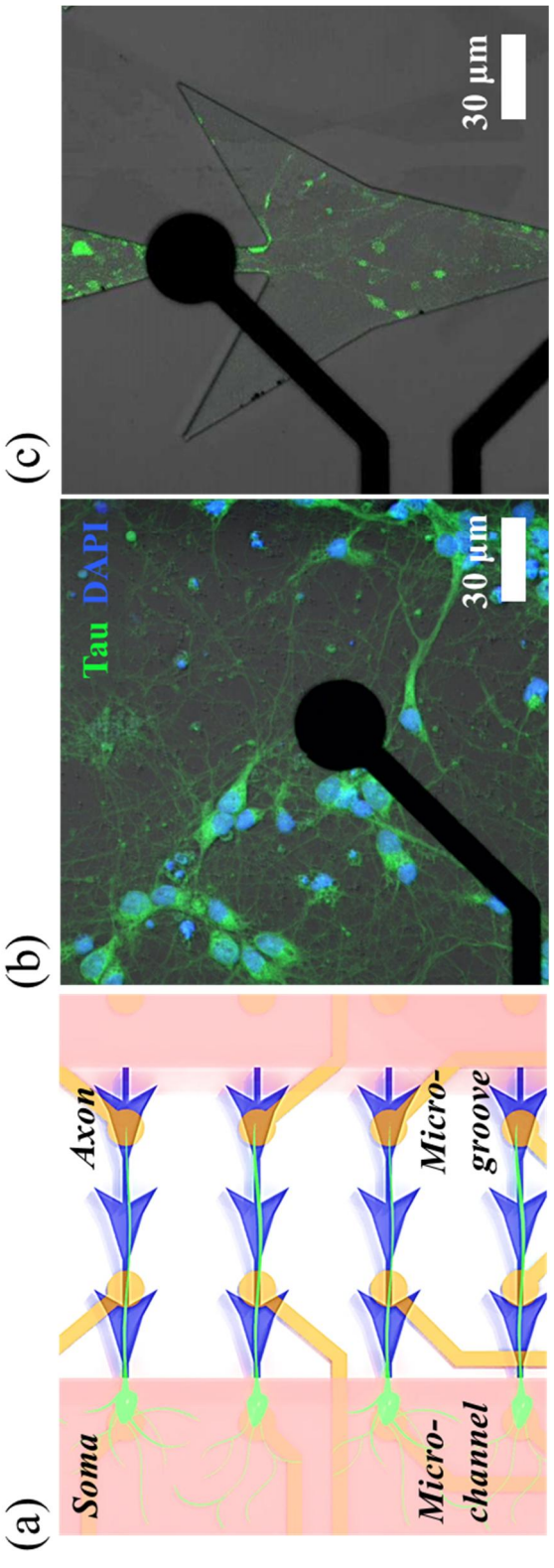

Figure 2-2. Diagram of neuron (a) and florescent images (b, c) in the microfluidic device coupled with MEA as previously published study in [55].

2.3 Chemicals

In this paper, we utilized two commercially available caged glutamates: MNI-caged glutamate [4-methoxy-7-nitroindolinyl-caged Glutamate, Tocris Bioscience, UK, **(Fig. 2-3-(a))**] and RuBi-caged glutamate [Ruthenium-bipyridine-trimethylphosphine-Glutamate, Abcam, USA, **(Fig. 2-3-(b))**]. Those were dissolved in a 100 mM and 10 mM distilled water respectively. And aliquots of each chemical solution were prepared to use small volumes at a time. Before the experiments, two chemical solutions were added to the experimental medium at the final concentration (MNI: 1, 2 and 4 mM, Rubi: 50, 100 and 200 μM). Final concentration of two chemicals was limited respectively with consideration for photochemical uncaging efficiency.

Absorption UV–visible spectra of MNI-caged glutamate (3 mM) and Rubi-caged glutamate (3 mM) in distilled water were measured by Fluorometer (Cary 5000, Varian, USA) in UNIST Materials Characterization Lab **(Fig. 2-4)**. The peak absorption of MNI-caged glutamate and of RuBi_caged glutamate appear as 1.4919 at 340 nm, and 1.3595 at 445 nm respectively, which two peak are displayed with blue and red circle **(Fig. 2-4)**. And absorbance for four center wavelength from which light source can emit is represented by asterisk '*'.

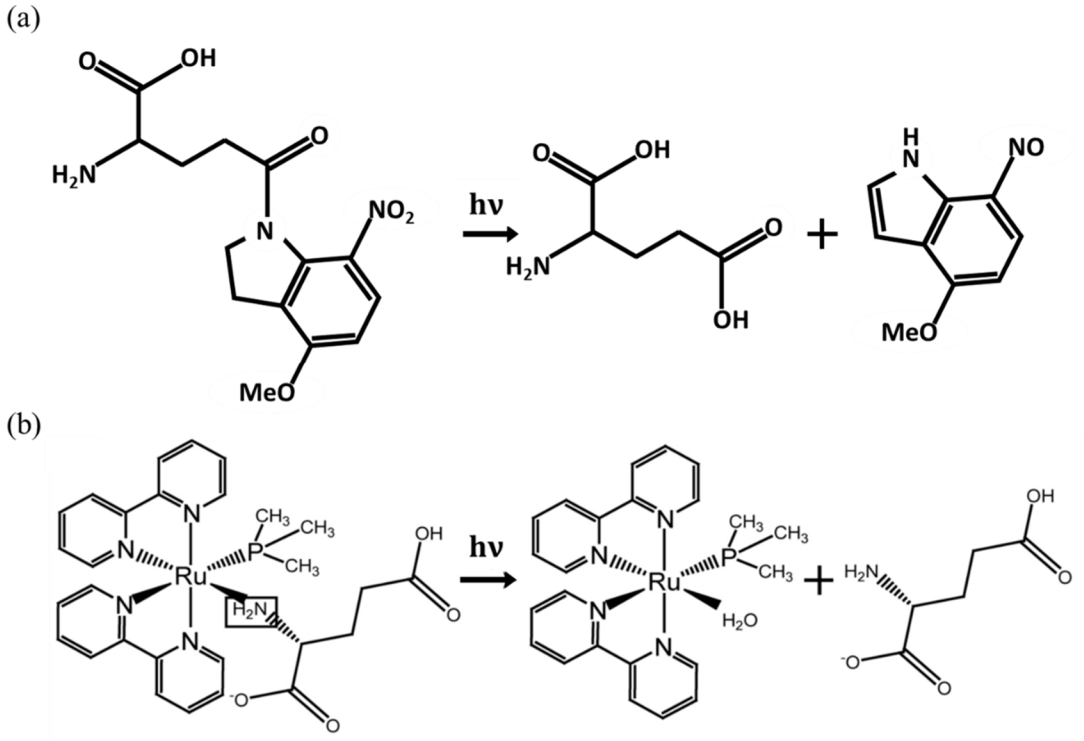

Figure 2-3. Structure of MNI-caged glutamate (a) and Rubi-caged glutamate (b) [24], and glutamate photo-release reaction to generate L-glutamate and by-product.

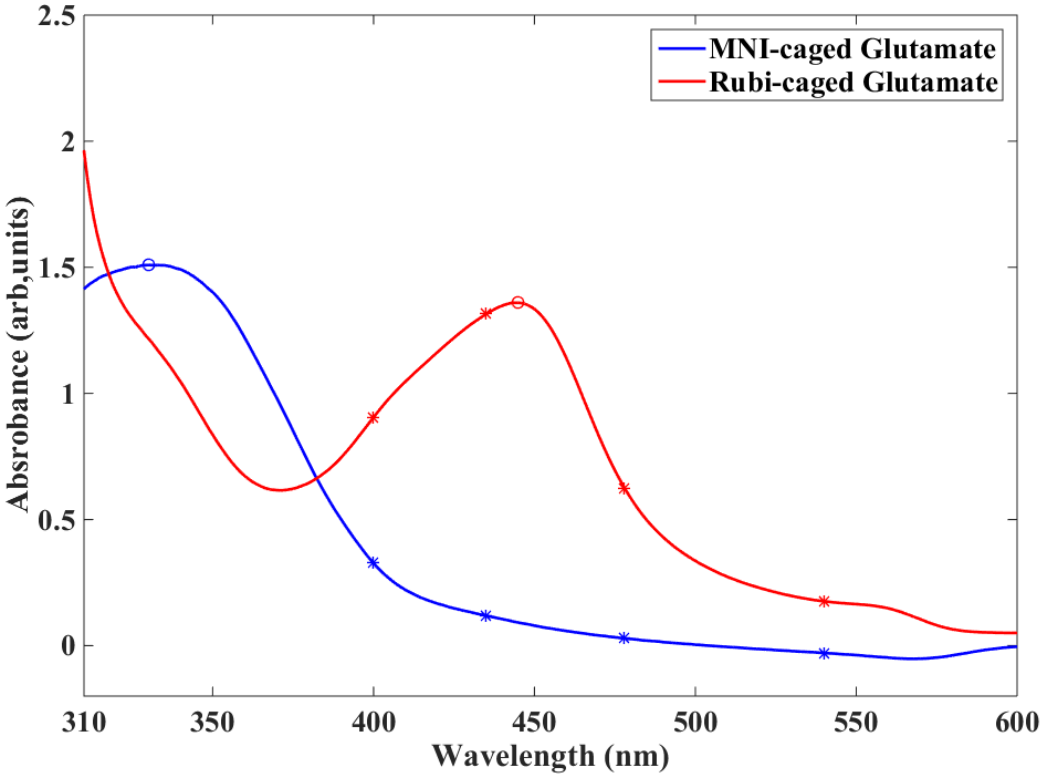

Figure 2-4. Absorption UV–visible spectra of MNI-caged glutamate (blue line) and Rubi-caged glutamate (red line) in distilled water. The peak absorbance (circle) for MNI and Rubi caged glutamate is at 340 nm and 445 nm. The absorbance (asterisk) for MNI and Rubi caged glutamate is shown about four wavelengths: 400, 435, 478, 540 (nm)

2.4 Neural recording system and data processing

For electrical recording, we utilized 60-channel extracellular recording system (USB-ME64, multichannel systems, Germany) and Microelectrode array (MEA, multichannel systems, Germany). Designed MEA in advance consisted of 8 × 8 or 6 × 10 array with a reference electrode such as Ch.15. And diameter of each electrodes was 30 μm and each distance of individual electrodes was 200 or 500 μm.

All experimental data were recorded at 10 kHz sampling rate from each channel. And then those data were filtered from 100 Hz to 3 kHz for elimination of chronic powerline (60 Hz) noise and low-frequency signal. The average noise level was less than ± 20 μV. Because all data from each 60 channel were necessary for this experiment, we extracted and analyzed only data from one channel of interest, which in neuronal excitation evoked in the response to photolysis of caged glutamate. Also for monitoring every optically-stimulus events, trigger signal from internal counter keep a record of starting time in total discrete-time data.

Analysis of spikes waveform and quantification of spikes characteristics, was carried out as follows.

The measured neural signals were converted into a file format processable with MATLAB (MathWorks, USA). A single electrode acquires electrical activity from more than one neuron due to densely distributed neurons with overlapping extracellular field potentials **[56]**. To minimize the number of overlapping extracellular action potentials, the measured data should be dealt with the spike sorting technique to extract the same spike waveform. Firstly, the spikes were detected by negative or positive amplitude thresholding at 5 ~ 10 **[57]**, and aligned to their peak values. Spike waveforms were cut out in the period of 5ms from 2 ms before and 3 ms after detected point. Secondly, wavelet transform was applied in extraction of distinctive features from the spike waveforms. And finally these features were classified by clustering of the spikes. As one of clustering methods, we selected Superparamagnetic Clustering (SPC) as further described in **[58]**. The spike sorting was executed and modified based on 'wave_clus' (Rodrigo Quian Quiroga, 2009). In summary, **Fig. 2-5** show outline of spikes detection and clustering method in our experiment result.

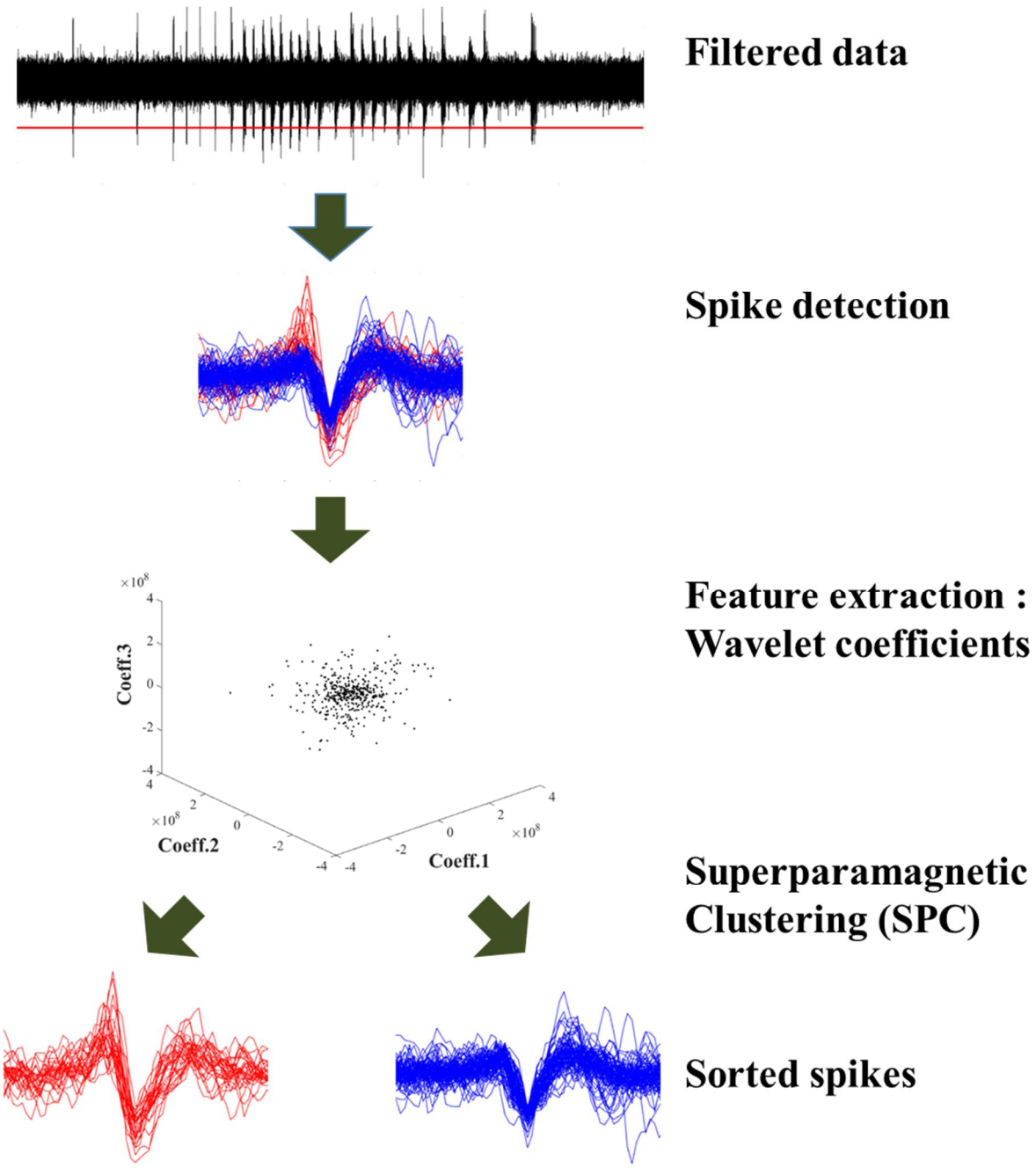

Figure 2-5. Outline of spikes detection and clustering method

2.5 Light source and LabVIEW software for optical stimulation

In this study, continuous UV-visible light ranging from 300 ~ 600 nm [SOLA Light Engine, Lumencor, USA, (**Fig.2-6-(b)**)] is used to investigate neuronal responses about photolysis of caged glutamate according to period of illumination, light intensity and wavelength. It could have five discrete spectral outputs colors: UV (400 nm), Blue (435 nm), Cyan (478 nm), Teal (515 nm), Green/Yellow (540 nm) and Red (630 nm) with regard to center wavelength. The spectral power distribution over the UV-visible spectrum from a source was measured by spectrometer (USB 4000, OceanOptics, USA) in **Fig.2-6-(a)**. Since each wavelength of different light have variation of maximum and minimum output of intensity, illuminating power was limited to 17.5 ~ 175 mW in this experiment

A LabVIEW based software was developed to control optical stimulus condition using serial communication between computer and light source **[Fig.2-6-(c)]**. In addition, internal counter transfer a trigger TTL (Transistor-Transistor Logic) signal to the recording system simultaneously for synchronization.

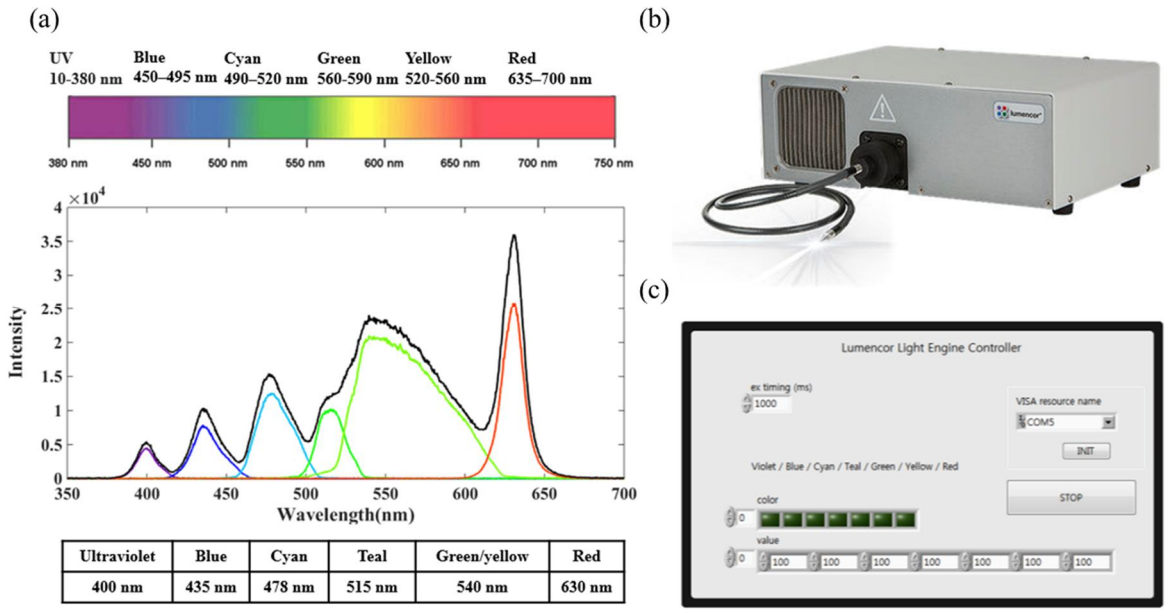

Ultraviolet	Blue	Cyan	Teal	Green/yellow	Red
400 nm	435 nm	478 nm	515 nm	540 nm	630 nm

Figure 2-6. Spectral power distribution over the UV-visible spectrum from light source (a). Actual image of it (b). Homemade LabVIEW GUI (c).

Chapter 3. Result.

Part. 1.

3. 1. 1. Photolysis of caged glutamate

We demonstrated the feasibility to stimulate the synaptic activation evoked by photo-release of L-glutamate from two caged glutamate according various stimulation condition. For example, **Fig. 3-1.** show raw data of photolysis of 1 mM MNI (**Fig. 3-1-(a, b))** with 87.5 mW light of 400 nm in duration of 500 ms, and 200 μM Rubi (**Fig. 3-1-(c, d))** with 52.5 mW light of 435 nm in duration of 500 ms. The raster plot in **(Fig. 3-1-(b, d))** signify each point of an action potential in the time scale as dot. All experiments were repeated 10 ~ 12 times in order to ensure a reliable reproducibility. In same protocol, we investigated neuronal responses including the number of spikes/s and latency depending on power, exposure and concentration as follows. In order to minimize biological variation in cell and experiment, we tried to acquire each data from the same sample about fixed stimulation condition.

Firstly, we measured the number of spikes according to various illuminating power (17.5 to 175 mW) and duration (50 to 500 ms) using 1 mM MNI (**Fig. 3-3.**) and 200 μM Rubi-caged glutamate (**Fig. 3-4**) with 400 and 435 nm wavelength of light respectively. Evoked spikes were counted for 1 second after stimulus onset and averaged by trial numbers. The number of spikes increased with high power and long duration in the MNI (0 ~ 16.3) and Rubi (1 ~ 24.5). Even though Rubi had lower concentration in cultured media than MNI, photochemical efficiency of Rubi may complement its deficiency, and produce more released glutamate resulting in high the number of spikes. Secondly, we assessed latency on the identical experimental conditions as described above. Latency usually stand for the delay between the stimulus onset and the beginning of the response **[59]**. It was also measured and averaged by the number of trials about MNI (**Fig. 3-5-(a)**) and Rubi-caged glutamate (**Fig. 3-5-(c)**). Also, it was determined to 1000 ms on several stimulation condition, on which the action potential was not evoked by the photolysis. In the both of two chemicals, the latency was in inverse proportion to illuminating power in MNI (197.1~321.4 ms) and Rubi (40.4~135.1 ms). This result indicate that high power per unit time reached quantity of released glutamate promptly enough to give rise to action potentials. In the Peri-stimulus time histogram (PSTH), the response time for 1 seconds was segmented by 25 ms, and the event of spikes in the period was divided by trial numbers (**Fig. 3-5-(b, d)**) under the same conditions in **Fig. 3-3** and **Fig. 3-4**. First response time by one-photon photolytic reaction by MNI, was delayed when compared to Rubi. Because quantum yield was measured by rate of reaction as previously described, and quantum yield (0.13) of Rubi is higher than that (0.085) of MNI. Thirdly, the high concentration of caged glutamate evoked more spikes as shown **Fig. 3-6** (MNI) and **Fig. 3-7** (Rubi).

Finally, our results suggested that illuminating power, duration, and concentration influence on the amount of released glutamate, which was revealed by investigating spikes/s and latency in response to photolysis.

3.1.2. Comparison of neuronal responses to photo-release of glutamate from caged glutamate with spontaneous glutamatergic synaptic activities

To examine the feasibility of synaptic activation by photo-release of glutamate, we conducted a series of experiments to compare neuronal responses to photo-released glutamate with spontaneous glutamatergic synaptic activities in cultured neurons. **Fig. 3-2-(a, d)** shows spontaneous and neuronal responses evoked in 4 mM MNI-glutamate and 100 μM Rubi-cage glutamate by 20 ms pulses at 52.5 mW of 400 nm light. **Fig. 3-2-(b, e)** shows spontaneous synaptic activities (blue) and **Fig. 3-2-(c, f)** shows neural activities by photo-released glutamate (red). Each experiment recorded electrical signals for 5 min, and separate the period including spontaneous activities from the total response time (1 seconds) after optically stimulation at 10 trials. Every evoked spikes in the same electrode channel were extracted and superimposed (Normal: 397, MNI: 76, Normal: 493, Rubi: 95).Signals in the MNI-cage glutamate have initial, positive peak of spike waveform. In contrast, those in the Rubi-cage glutamate have dominant, negative peak. However, such difference of extracellular waveform between them was caused by the electrode position relative to part of the recorded cell **[60]**, but not by type of chemicals. There is no a remarkable disparity in waveform between spontaneous activities and optically evoked extracellular activities in all cases of MNI and Rubi-caged glutamate.

Based on extracted every spikes, we could quantify averaged minimum, maximum and peak-to-peak values of each spike amplitude, as shown **Table 3-1**. Representatively, the peak-to-peak value of spike amplitude by photolysis of MNI is 128.76 ± 2.277 μV, higher than that of the normal (120.7 ± 1.020 μV). In a while, the peak-to-peak value (Rubi, 109.2 ± 1.661) is lower than that of (114.4 ± 0.583 μV). Minimum, maximum and peak-to-peak values reveal no significant variation (< ± 6.740 %) between synaptic activities and neural activities by photolysis of both of two chemicals.

In terms of waveform and peak-to-peak value, negligible distinctions between spontaneous activities and optically evoked extracellular activities indicate that the same mechanism is applied in both of them for events in an action potential.

	MNI		**Rubi**	
	Normal (397)	Stimulation (76)	Normal (493)	Stimulation (95)
Min value	- 72.7 ± 0.669	- 77.6 ± 1.412	- 38.1 ± 0.174	- 37.1 ± 0.540
Max value	48.0 ± 0.395	51.2 ± 1.014	76.3 ± 0.488	72.1.1 ± 1.281
Peak-to-peak	120.7 ± 1.020	128.76 ± 2.277	114.4 ± 0.583	109.2 ± 1.661

Table 3-1. Comparison of spike amplitude (unit: μV) between spontaneous action potential and neural activities evoked by photolysis of caged glutamate

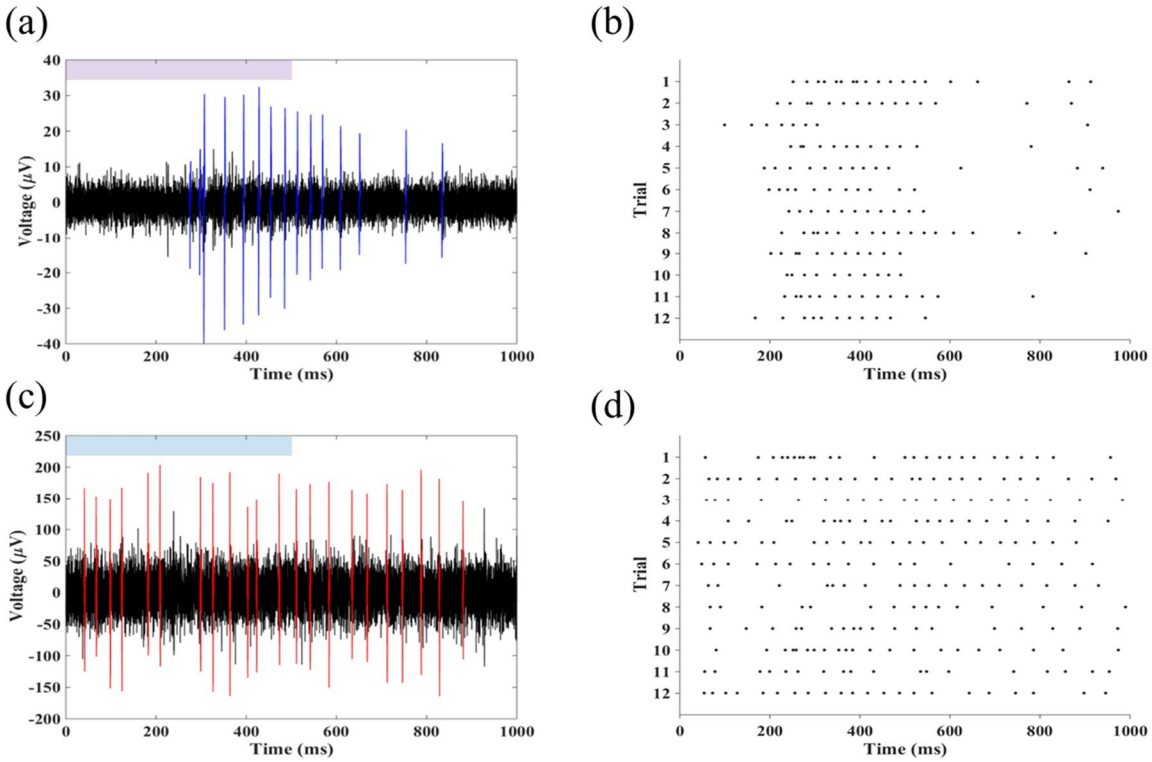

Figure 3-1. The raw data and raster plot of the neuronal signals evoked by photolysis of MNI-caged and Rubi-caged glutamate. Photolysis of MNI-caged glutamate (a) and Rubi-caged glutamate (c) evoke the neuronal signals. Spike raster plots of MNI-caged glutamate (b) and Rubi-caged glutamate (d) represent reproducibility about 12 trials.

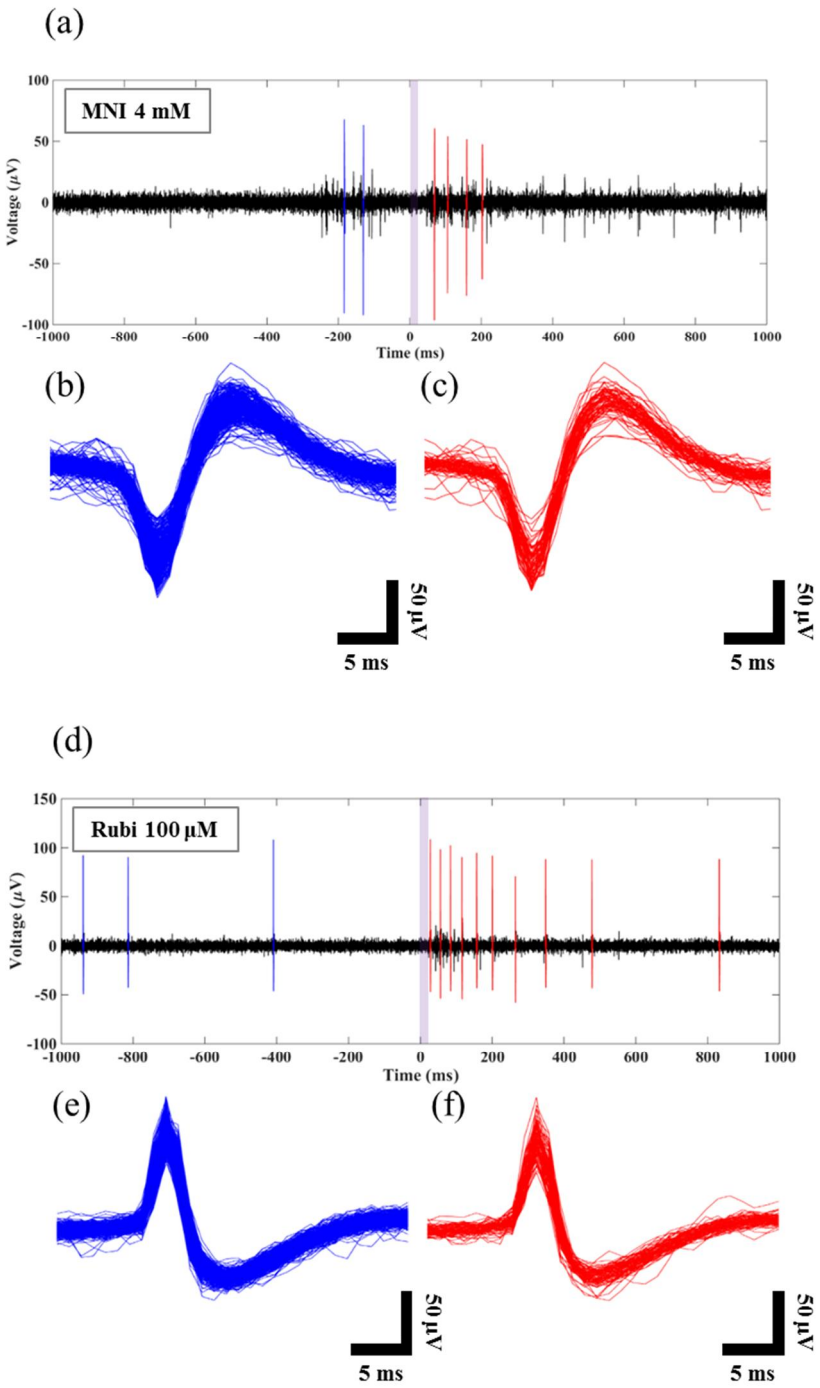

Figure 3-2. Comparison of spikes waveforms of spontaneous excitatory post-synaptic activities with neuronal activities evoked by photolysis of caged glutamate. Every evoked spikes of spontaneous signals (blue) (MNI (b), n=397; Rubi (e), n=493**)** and electrical activities (red) (MNI (e), n=76; Rubi (f), n=95**)** by photo-released glutamate about 10 trials, were measured and aligned**.**

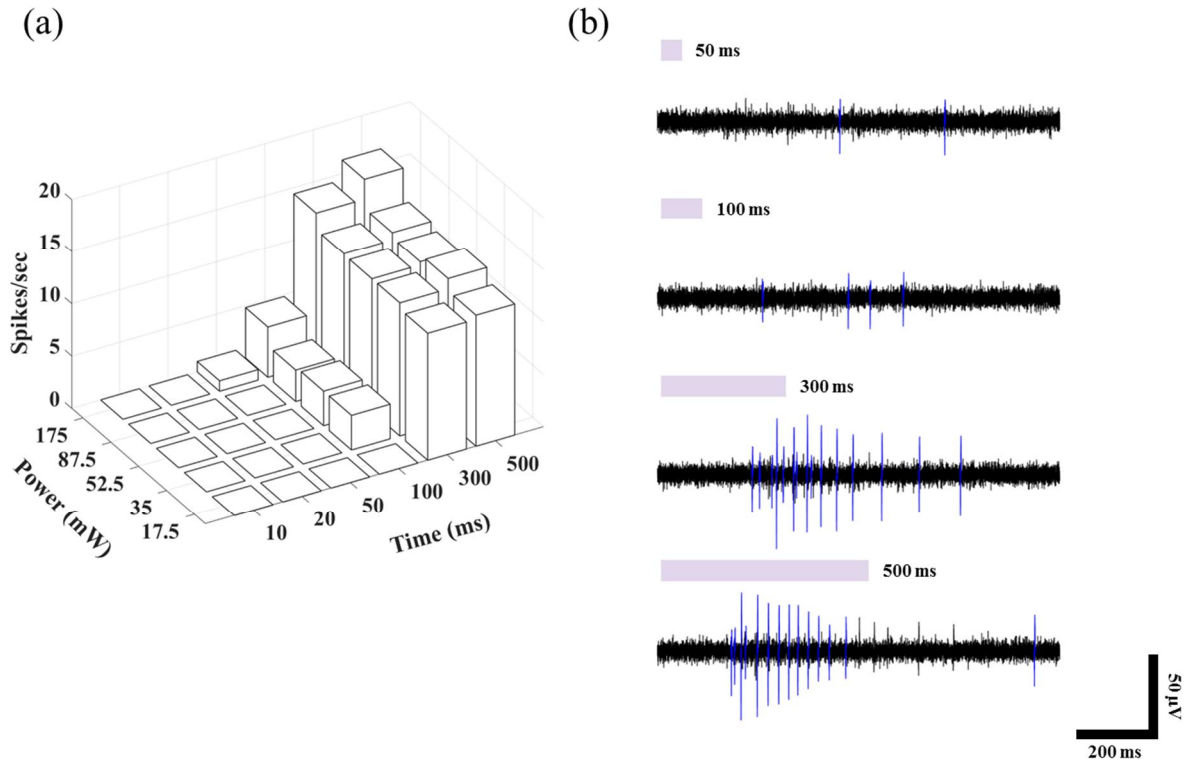

Figure 3-3. Variation in the number of spikes per sec with regard to illuminating power and duration by photolysis of MNI-caged glutamate (1 mM). (a) The number of spikes increase with high power (17.5 to 175 mW) and long illuminating time (50 to 500 ms). The number of spikes is mostly depends on illuminated time. (b) Neuronal signals depending on illuminated time from 50 to 500 ms.

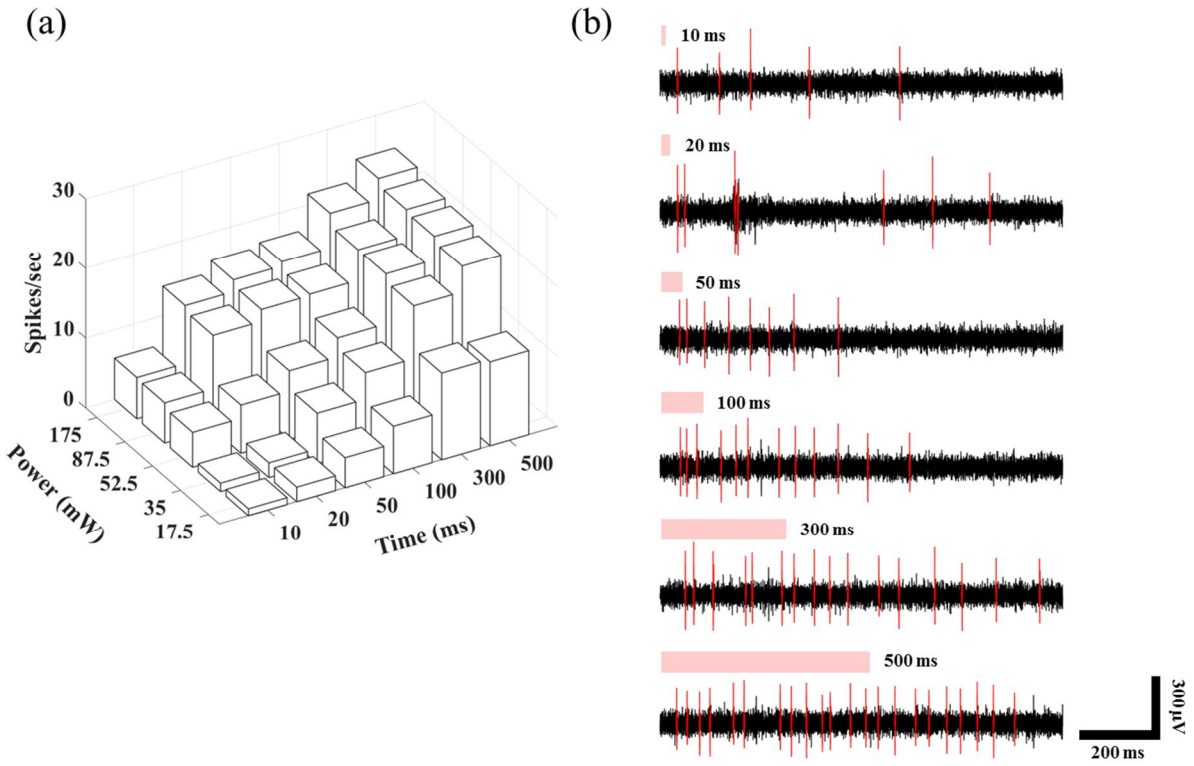

Figure 3-4. Variation in the number of spikes per sec with regard to illuminating power and duration by photolysis of Rubi-caged glutamate (200 μm). (a) The number of spikes increase with high power (17.5 to 175 mW) and long illuminated time(50 to 500 ms), and the number of spikes is mostly depends on illuminated time in accordance with the result of MNI-caged glutamate. (b) Neuronal signals depending on illuminated time from 10 to 500 ms.

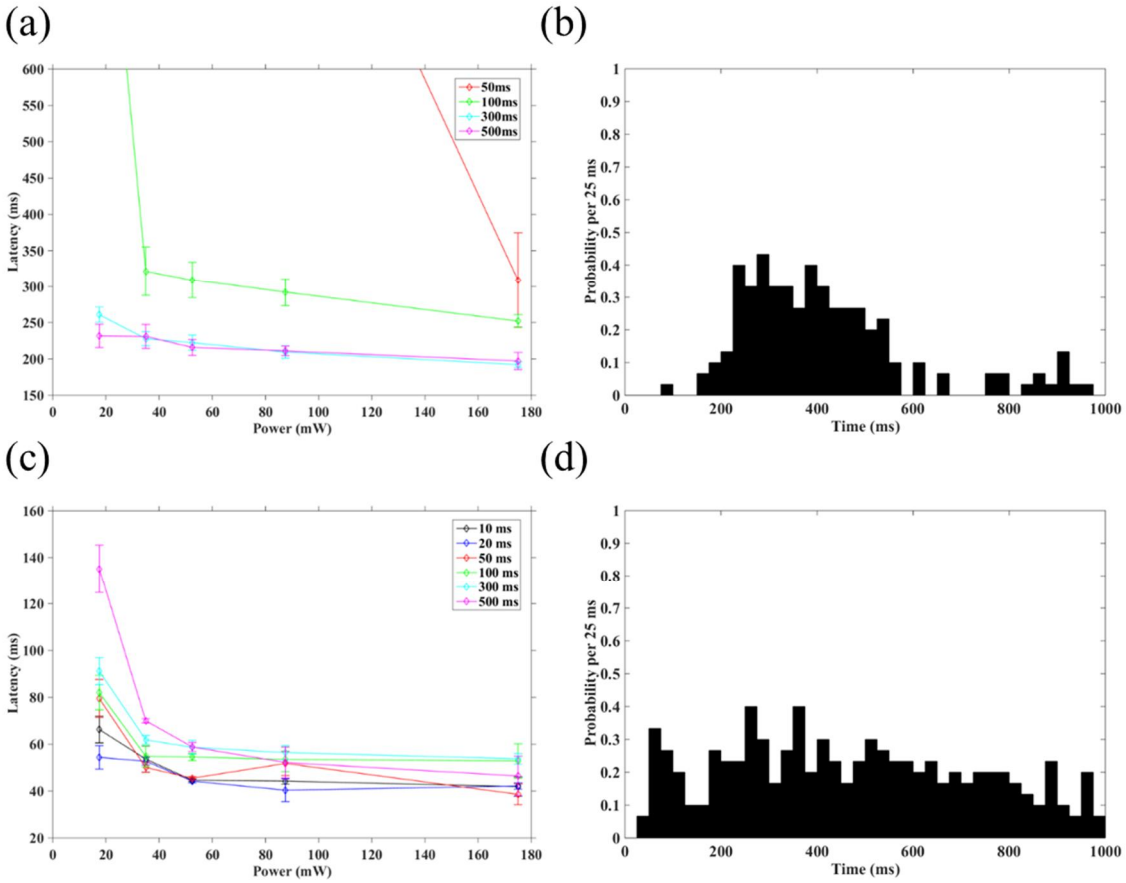

Figure 3-5. Variation in the latency with regard to illuminating power and duration by photolysis of MNI-caged and Rubi-caged glutamate.

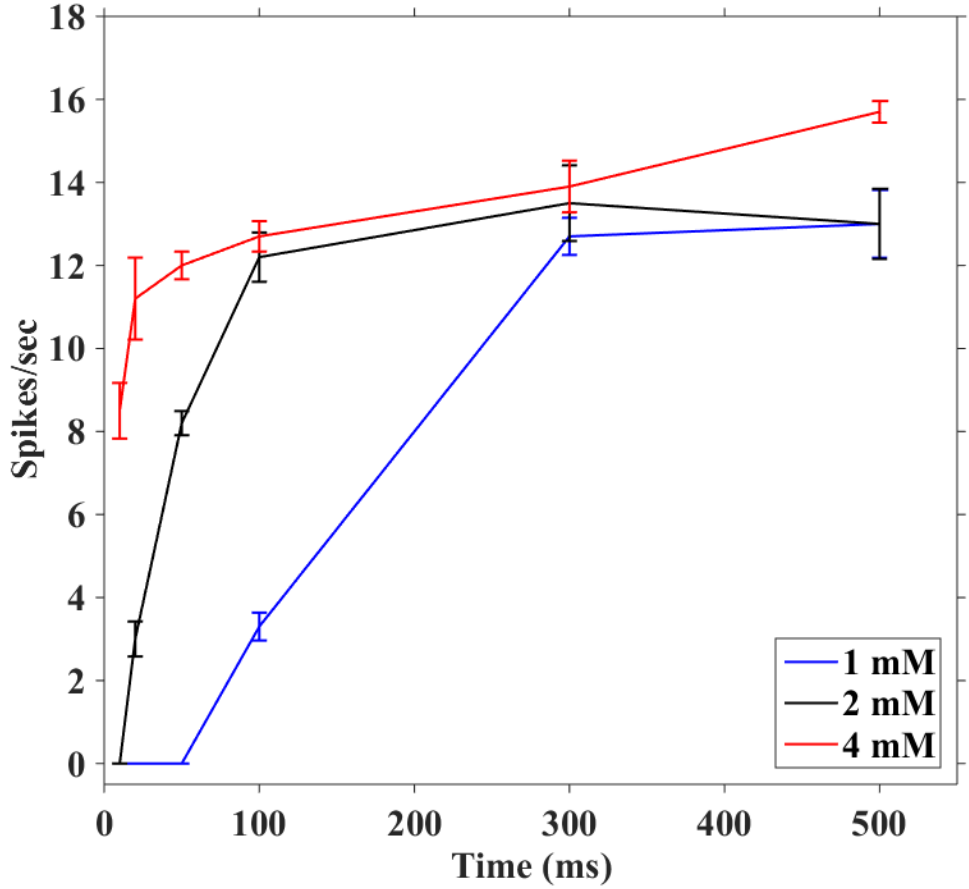

Figure 3-6. Dependency of the evoked spikes on concentration of MNI-caged glutamate with 400 nm light of 52.5 mW.

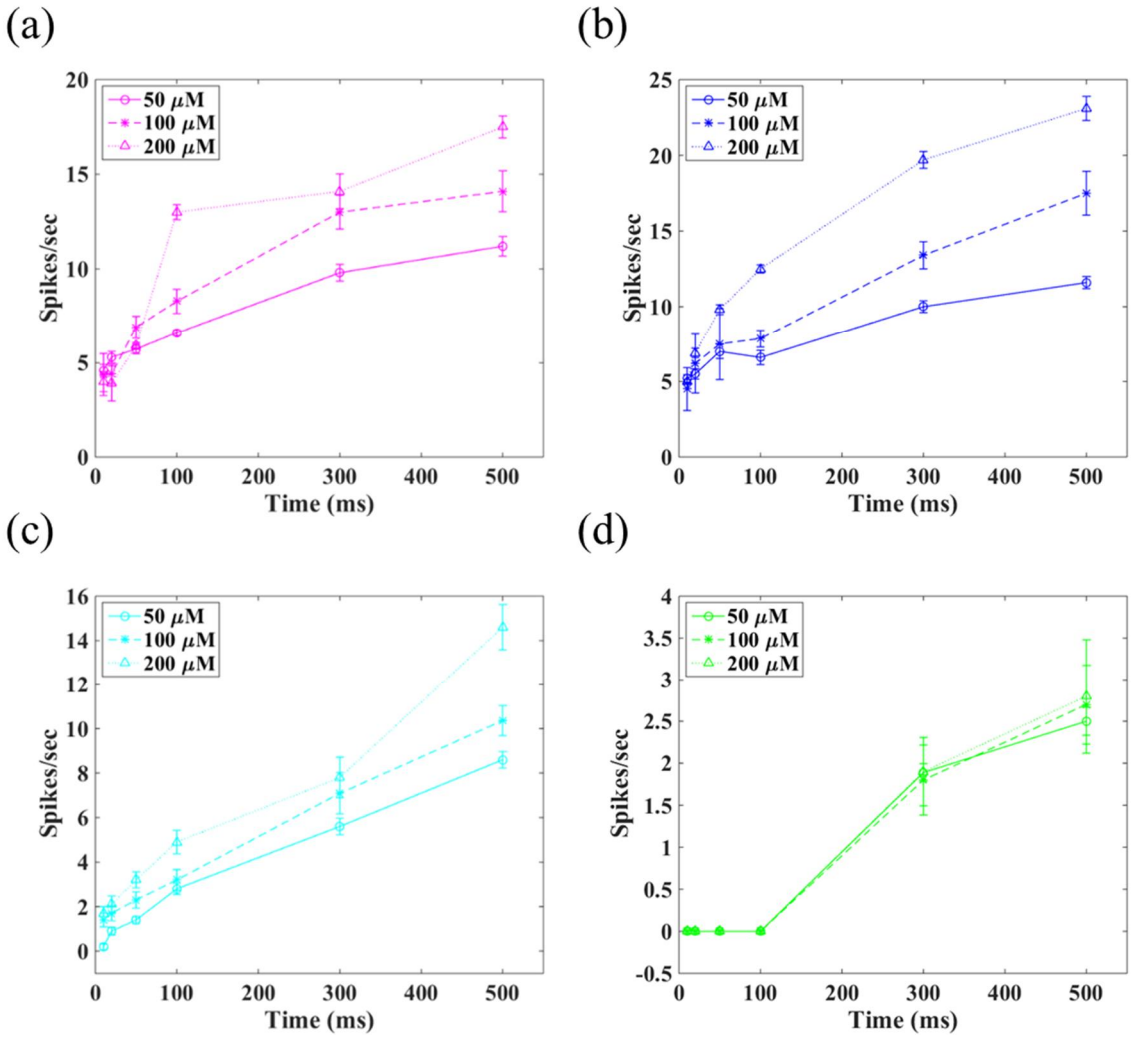

Figure 3-7. Dependency of the evoked spikes on concentration of Rubi-caged glutamate with 400 nm (a), 435 nm (b), 478 nm (c) and 540 nm (d) light of 52.5 mW.

Part. 2.

3. 2. 1. Numerical analysis of the amount of released glutamate for photolysis of caged glutamate

$$\text{Uncaged glu.}(moles) \approx \text{M} \times I(\frac{quanta}{m^2 s}) \times \text{DT(s)} \times \varepsilon(\frac{1}{M\ cm}) \times \Phi(\frac{number\ of\ moles\ converted}{number\ of\ quanta\ absorbed}) \times \text{V}(ml)$$

Formula 1. Estimated amount of released glutamate by photolysis

On the basis of the result in Part.1, we can formulate a new equation (**Formula 1.**) which establishes proportionality relationship between amount of released glutamate and photo-stimulation condition. All abbreviation and symbols related this formula are described in **Table 3-2**. The amount of released glutamate may be affected by the concentration, extinction efficiency and quantum yield of caged glutamate, but also optical stimulation conditions such as illuminating power, duration and uncaging volume. Since difficulty in direct measurement of released glutamate in single-molecule scale, this amount is verified by the neuronal response to photolysis of caged glutamate in experimental result. Several of reasonable assumptions are essential for acceptance of this equation. It is assumed that only released glutamate have effect on synaptic activation disregarding diffusion of the free glutamate and stimulation position related to distribution of excitatory glutamatergic receptor.

Individual term related to this is described in more detail as followed, and numerical simulation proceeds with MATLAB.

Concentration(M)	Intensity(mW)	Duration Time(s)	ε ($M^{-1}cm^{-1}$)	Φ(moles per Einstein)	Volume (ml)
Glutamate concentration	quanta $s^{-1}m^{-2}$	Exposure time	Extinct coefficient	Quantum yield	The uncaging volume

Table 3-2. Abbreviation and symbols related to formula 1.

Illuminating power

The intensity of radiated flux emitted from the light source is normally expressed in terms of power as the basic unit 'watt per unit cross-section (J s^{-1})' **[61]**. Through the quantum theory applying in photochemistry, the unit of light energy is summation of the quantum of light or photon **[62]**. With the wavelength of absorbed light, Intensity I (mW) could be converted to quanta $m^{-2}s^{-1}$ by Formula 2 **[61]**.

$$I = 5.03 \times 10^{24} \times \lambda\ (nm) \times \text{power}\ (watt) = \text{quanta}\ s^{-1}m^{-2}$$

Formula 2. Unit conversion of light intensity from power to quanta $s^{-1}m^{-2}$ [61]

Quantum yield

Since quantum yield in every single wavelength have been not reported yet and direct measurement of it, as previously above overview, is painful, quantum yield is assumed as a constant of 0.085 (MNI) and 0.13 (Rubi) in **Table1-1.**

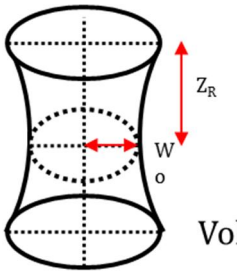

$$Wo = 1.22 * \lambda \frac{1}{2NA}$$

$$Z_R = \frac{\pi Wo^2}{\lambda}$$

$$\text{Volume } (V) = \frac{8}{3}\pi W_o{}^2 Z_R = \frac{8}{3\lambda}\pi^2 W_o{}^4$$

Figure 3-8. Calculation of the uncaging volume.

Where Wo = Beam radius at focus, ZR = Rayleigh range, N.A = Numerical aperture.

The photolysis stimulation geometry was complicated, as involved in both the uncaging geometry and the diffusion of the free compound. For concise assumption, the uncaging volume is estimated simply by two terms: beam radius and Rayleigh range from Gaussian beam optics. Beam radius (Wo), Gaussian laser beam waist at focus, is calculated with a given wavelength and a numerical aperture (N.A) defined as the range of acceptance and divergence angle. In all experiment and numerical simulation, 0.7 N.A 60x objective lens was utilized. The Rayleigh length (Z_R) is the distance along the propagation direction of a beam from the focus to the place where the beam radius spreads by a factor of $\sqrt{2}$ **[63]**. The hyperbolic uncaging volume is calculated by partial integration of cross section in the range of Rayleigh length.

Numerical analysis of released glutamate about extinction coefficient and wavelength

The Formula 1 for estimated amount of released glutamate increase depending on extinction coefficient for each of the chemicals, and fourth power of wavelength, as shown in **Fig. 3-9-(a, MNI)** and **Fig. 3-9-(b, Rubi)** as logarithmic scales. Because extinction coefficient of two chemicals specify measured absorbance according to wavelength, **Fig. 3-9-(a, MNI)** and **Fig. 3-9-(b, Rubi)** display a similar tendency between the released glutamate and extinction coefficient against wavelength. In addition, fourth power of wavelength was be concerned in the conversion of illuminating power and volume in this formula.

Numerical analysis of released glutamate about illuminating power, duration and concentration

Fig. 3-10 show the result of numerical analysis of released glutamate as variation of illuminating power (0 ~ 175 mW) and duration (0 ~ 500 ms) at 400 nm wavelength and the same concentration (200 μM) of MNI-caged **(Fig. 3-10–(a))** and Rubi-caged glutamate **(Fig. 3-10–(b)).** Simulated amount of glutamate in Rubi is bigger than that in MNI by a factor of 4.24 because of photochemical efficiency $\varepsilon \cdot \Phi$. Also, concentration have effect on released glutamate shown like **(Fig. 3-10–(c, d)).**

3. 2. 2. Demonstration of numerical analysis of the amount of released glutamate for photolysis of MNI and Rubi-caged glutamate

In order to demonstrate **Formula. 1** about the amount of released glutamate, we compared the activated response with calculated amount of released glutamate with different parameters. And finally we established a new equation to elucidate relationship between measured spikes and the estimated amounts of released glutamate.

Before the experiment, we had to seek stimulation conditions in practice due to relatively low photochemical efficiency of MNI-caged glutamate compared to Rubi. To find out threshold boundary, gradual increase of power (17.5~175 mW), duration (0 ~500 ms) and concertation (1, 2, 4 mM) with 400 nm light, was applied until even one spike appeared (**Fig. 3-10-(a)**). The area toward bottom left of threshold boundary is impossible to evoke action potential by photolysis, and by contrast, the other toward upper right of it is possible. Based on exploited stimulation conditions, light energy by multiplication of power and duration was shown in **Table. 3-3** and, additionally multiplying concentration to that in **Table. 3-4**. We could make certain that those values converge (3000 ~ 3964.4(10^{-6} J·M)) to some extent. Moreover, the amount of released glutamate was calculated and averaged as constant 0.5502 ± 0.0128 (mmoles) by **Formula. 1 (Fig. 3-10-(b))**.

To investigate how wavelength in **Formula. 1** have effects on neuronal response and released glutamate for photolysis of two caged glutamate, we conducted series of experiments with four wavelength (400, 435, 475 and 540 nm). **Fig. 3-11 (MNI)** and **Fig. 3-12 (Rubi)** revealed that the number of spikes/s has similar tendency to estimated glutamate according to different wavelengths of light. It may be because each caged glutamate have different absorption UV–visible spectra and proportionality of wavelength.

Finally, the number of spikes/s was plotted against estimated amount of released glutamate by photolysis of MNI (blue △) and Rubi-caged glutamate (Rubi: red ▽) as shown in **Fig. 3-13-(a)**. The equation **(Fig. 3-13-(b))** for the fitted line to the data was deduced using Curve Fitting Toolbox in MATLAB. The coefficients of ‘a’ and 'b’ in the **Fig. 3-13-(b)** are determined by fitting this equation to the measured data to give the least squared error. Evaluation of precision to the fitted line was conducted by R-squared (R^2) calculated as 0.4826 (MNI) and 0.9942 (Rubi). The symbol of ‘a’ in this formula determines the saturation of the number of spikes, and the symbol of ‘b’ contributes to gradient of graph in the initial state. This result reveals relationship between measured spikes and the estimated amounts of released glutamate.

$$\text{Uncaged glutamate (moles)} \approx$$

$$M \times \boxed{5.03 \times 10^{24} \times \lambda\,(nm) \times \text{power}} \times \text{DT(s)} \times \boxed{\varepsilon\left(\frac{1}{M\,cm}\right)} \times \Phi\left(\frac{number\ of\ moles\ converted}{number\ of\ quanta\ absorbed}\right) \times \boxed{\frac{8}{3}\pi^2 \times \left(\frac{1.22}{2NA}\right)^4 \times \lambda^3}$$

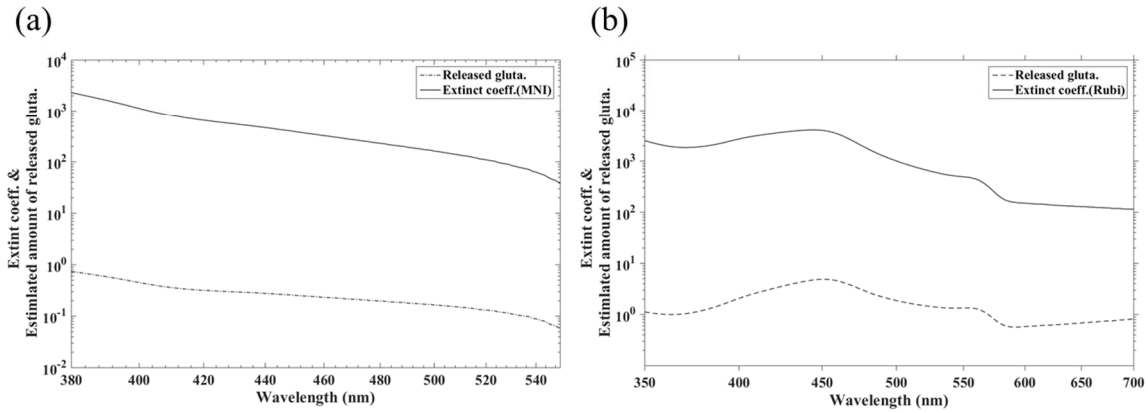

Figure 3-9. Assessment of estimated amount of released glutamate against extinct coefficient and wavelength. Comparison of estimated amount of released glutamate with extinction coefficient of MNI-caged glutamate (a) and Rubi-caged glutamate (b). Estimated amounts of released glutamate depend on extinction coefficient for each of the chemicals, and fourth power

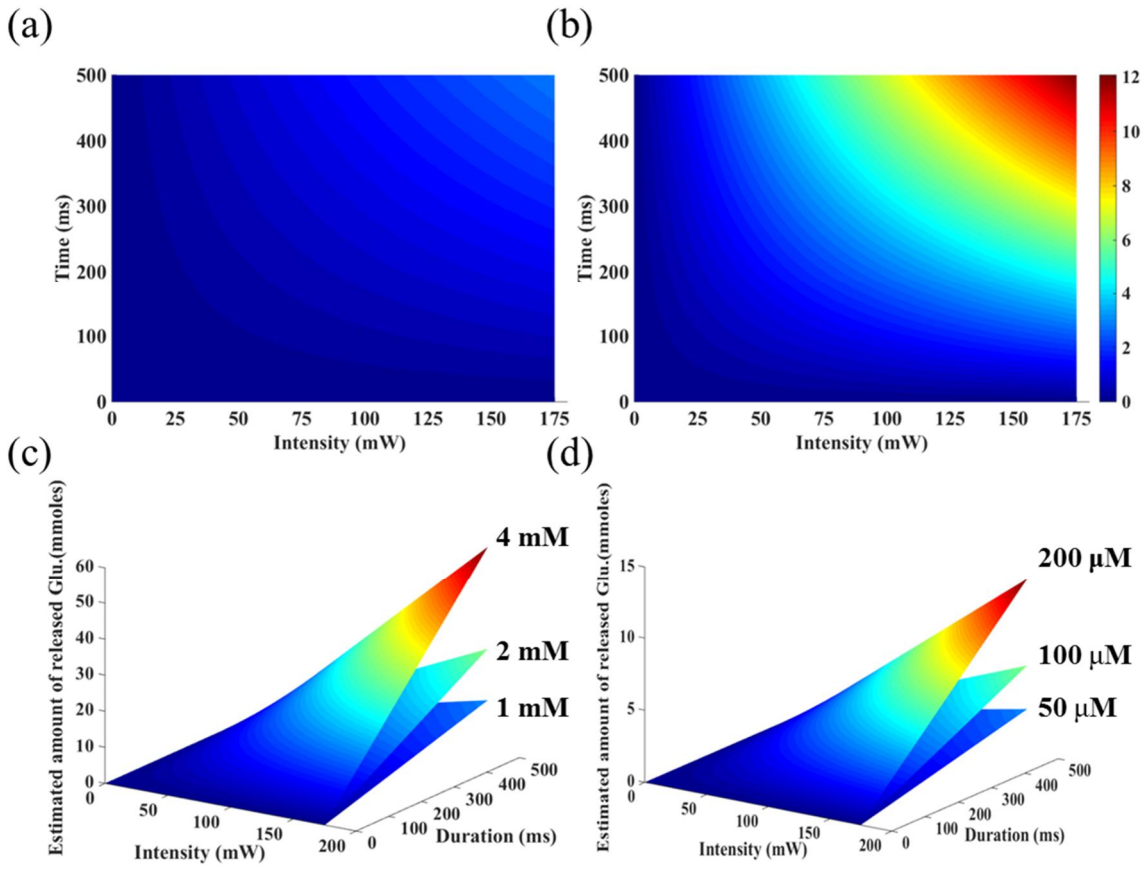

Figure 3-10. Numerical modeling of released glutamate based on Formula 1.

Estimated amounts of uncaged glutamate are calculated with illuminating power and duration time, on the same concentration of MNI-caged (a) and Rubi-caged glutamate (b). Each of the simulated amount of released glutamate is displayed for several concertation of MNI-caged (c) and Rubi-caged glutamate (d).

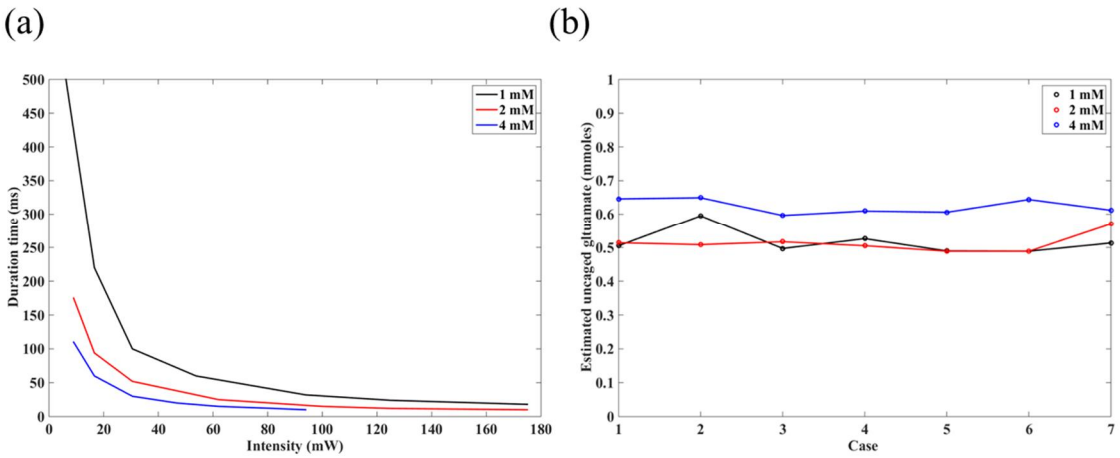

Figure 3-11. Threshold for photolysis of MNI-caged glutamate (a), and estimated amount of uncaged glutamate requisite for neural activities (b).

	Power (mW) × Time (ms)						
1 mM	6.20 * 500	16.6 * 220	30.5 * 100	53.8 * 60	93.9 * 32	125 * 24	175 * 18
2 mM	9.01 * 175	16.6 * 94	30.5 * 52	62 * 25	100 * 15	125 * 12	175 * 10
4 mM	9.01 * 110	16.6 * 60	30.5 * 30	46.7 * 20	62 * 15	82.3 * 12	93.9 * 10

Table 3-3. Multiplication of power (mW) × duration (ms)

	Power (mW) × Time (ms) × Concentration of caged glutamate (M)						
1 mM	3100	3652	3050	3228	2817	3000	3500
2 mM	3153.5	3120.8	3172	3100	3000	3000	3500
4 mM	3964.4	3984	3660	3740.8	3720	3951.36	3756

Table 3-4. Multiplication of power (mW) × duration (ms) × concentration of caged glutmate (M)

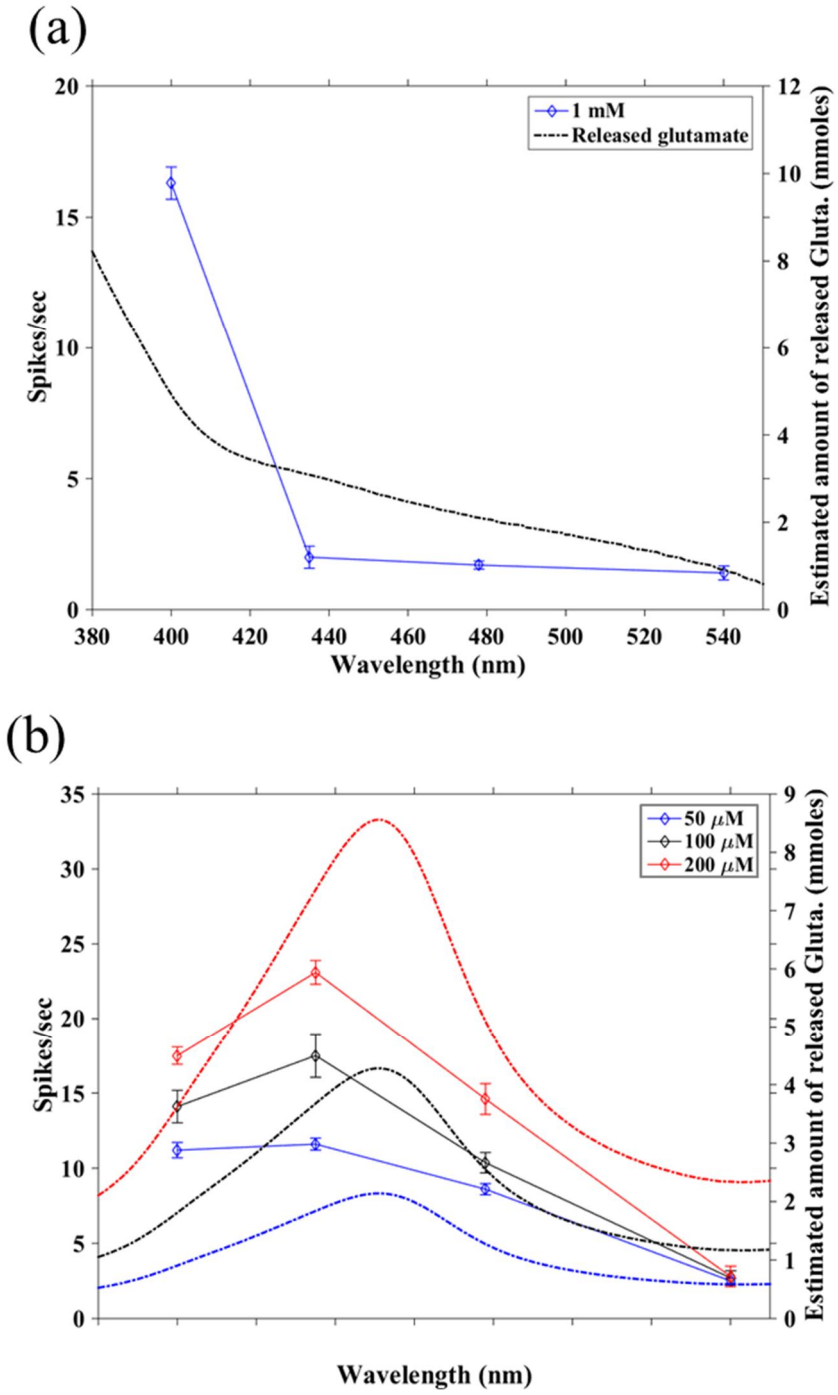

Figure 3-12. Plotting of the number of spikes/s against estimated amount of released glutamate by photolysis of MNI (a) and Rubi-caged glutamate (b) according to their wavelength.

(a)

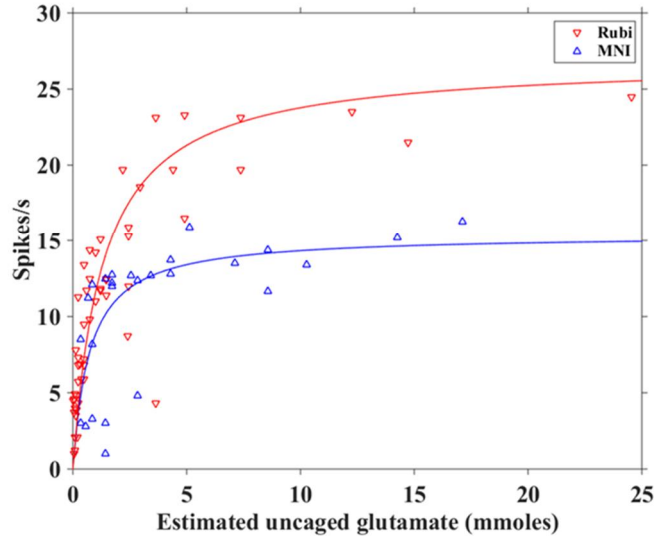

(b)

$$Trend\ line = \frac{a}{1 + \frac{b}{x}}$$

	MNI	Rubi
a	15.38	26.89
b	0.7369	1.312
R^2	0.4826	0.9942

Figure 3-13. Plotting of the number of spikes/s against estimated amount of released glutamate by photolysis of MNI (blue) and Rubi-caged glutamate (a). The best fitting equation to the measured data elicits the relation between released glutamate and the number of spikes (b).

Chapter 4. Discussion and conclusion

There are several differences between excitatory post-synaptic activities and response by photolysis, although having no a certain disparity of waveform, and peak-to-peak value between them. Spontaneous activities revealed that the positive or negative peak was irregular **Fig 3-2-(a, d).** On the other hand, the peak of neuronal activities by photolysis showed higher or lower peak appeared as first response, and gradually decreased in both chemicals **Fig 3-2-(a, d).** Also, the previous studies about rat cerebellum in *in vitro* brain slice, reported that the peak of the photolysis current is broader and the decline slower than the synaptic events **[64].** Redundant free glutamate released by intense photolysis may generate highest and lowest peak. And diffusion of the released glutamate in extracellular environment, interfered with cell's repolarization for a while. In addition, bursts of spikes didn't give arise in case of photolysis response, but those often appeared in spontaneous post-synaptic activities [data not included].

In order to investigate the result in **Fig. 3-13** in more detail, we extracted several of data and rearranged according to concentration of MNI **(Fig. 4-1-(a))** and Rubi **(Fig. 4-1-(a))**. In case of violet (400 nm) or blue light (435 nm) in the range of high extinction coefficient in both chemicals, all line was well-converged. In contrast, it showed great difference in cyan (478 nm) and green light (540 nm) with low extinction coefficient. Such difference in cyan and green light was caused by our assumption that quantum yield have constant value. Also increase of estimated amount to fourth power of wavelength compensated low extinction in those two light resulting in bigger amount of uncaging than in real. To minimize this error, it is necessary to measure quantum yield about each wavelength and reconsider the definition of the uncaging volume.

In this study, we studied photochemical properties of MNI and Rubi-caged glutamate in cultured hippocampal neuron on MEA combined with microfluidic chips. In order to comprehend photochemical properties (extinction coefficient and quantum yield) of caged compound, various optical stimulation condition is applied in experiments. Comparing extracted waveforms in both of chemicals, it is verified that response of photolysis correspond to glutamatergic activities. Also, the number of evoked spikes per sec was dependent on wavelength, illuminating power, exposure duration and concentration of caged compounds. Furthermore, the first response time from onset was in inverse proportion to illuminating power. We demonstrated that three optical factors and concentration had influenced on the amount of released glutamates. Finally, we suggested a new and empirical equation, which can quantify the uncaging with the known photochemical characteristic. Numerical modeling of the uncaging could elucidate neural response evoked by uncaged glutamate. Therefore, we demonstrated the potential of numerically quantification of the amount of various released compounds.

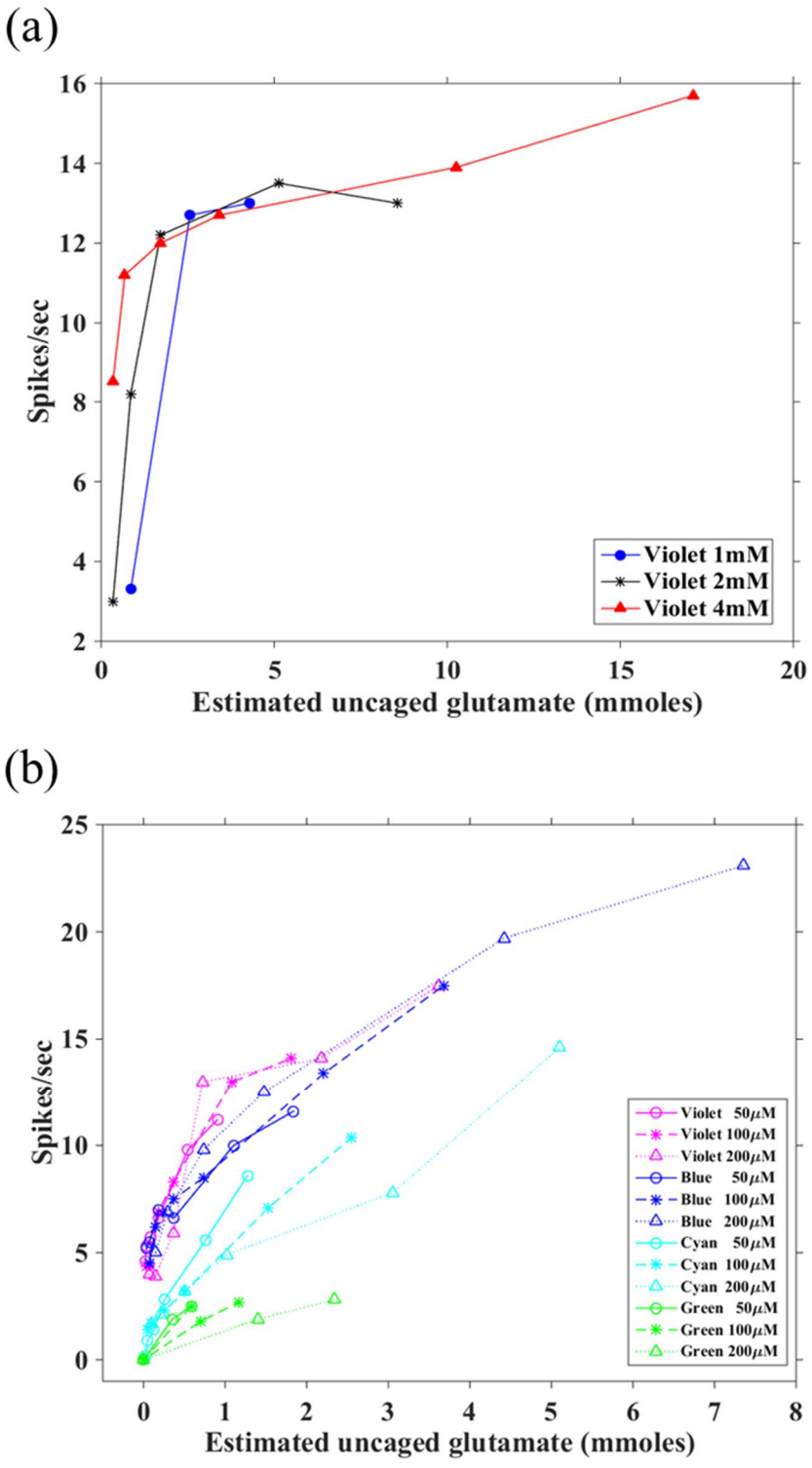

Figure 4-1. Plotting of the number of spikes/s against estimated amount of released glutamate by photolysis of MNI (a) according to its concentration, and Rubi-caged glutamate (b) according to its concentration and wavelength.

Reference

[1]. Engels, J., & Schlaeger, E. J. (1977). Synthesis, structure, and reactivity of adenosine cyclic 3', 5'-phosphate-benzyltriesters. Journal of medicinal chemistry, 20(7), 907-911.

[2]. Kaplan, J. H., Forbush III, B., & Hoffman, J. F. (1978). Rapid photolytic release of adenosine 5'-triphosphate from a protected analog: utilization by the sodium: potassium pump of human red blood cell ghosts. Biochemistry, 17(10), 1929-1935.

[3]. Mayer, G., & Heckel, A. (2006). Biologically active molecules with a “light switch”. Angewandte Chemie International Edition, 45(30), 4900-4921.

[4]. Tsien, R. Y., & Zucker, R. S. (1986). Control of cytoplasmic calcium with photolabile tetracarboxylate 2-nitrobenzhydrol chelators. Biophysical journal, 50(5), 843.

[5]. Adams, S. R., Kao, J. P., Grynkiewicz, G., Minta, A., & Tsien, R. Y. (1988). Biologically useful chelators that release Ca2+ upon illumination. Journal of the American Chemical Society, 110(10), 3212-3220.

[6]. Ellis-Davies, G. C. R., & Kaplan, J. H. (1988). A new class of photolabile chelators for the rapid release of divalent cations: generation of caged calcium and caged magnesium. The Journal of Organic Chemistry, 53(9), 1966-1969.

[7]. Ellis-Davies, G. C., & Kaplan, J. H. (1994). Nitrophenyl-EGTA, a photolabile chelator that selectively binds Ca2+ with high affinity and releases it rapidly upon photolysis. Proceedings of the National Academy of Sciences, 91(1), 187-191.

[8]. Walker, J. W., Somlyo, A. V., Goldman, Y. E., Somlyo, A. P., & Trentham, D. R. (1987). Kinetics of smooth and skeletal muscle activation by laser pulse photolysis of caged inositol 1, 4, 5-trisphosphate. Nature, 327(6119), 249-252.

[9]. Walker, J. W., Gilbert, S. H., Drummond, R. M., Yamada, M., Sreekumar, R., Carraway, R. E., & Fay, F. S. (1998). Signaling pathways underlying eosinophil cell motility revealed by using caged peptides. Proceedings of the National Academy of Sciences, 95(4), 1568-1573.

[10]. Ghosh, M., Song, X., Mouneimne, G., Sidani, M., Lawrence, D. S., & Condeelis, J. S. (2004). Cofilin promotes actin polymerization and defines the direction of cell motility. Science, 304(5671), 743-746.

[11]. Milburn, T., Matsubara, N., Billington, A. P., Udgaonkar, J. B., Walker, J. W., Carpenter, B. K., ... & Denk, W. (1989). Synthesis, photochemistry, and biological activity of a caged photolabile acetylcholine receptor ligand. Biochemistry, 28(1), 49-55.

[12]. Ando, H., Furuta, T., Tsien, R. Y., & Okamoto, H. (2001). Photo-mediated gene activation using caged RNA/DNA in zebrafish embryos. *Nature genetics*, *28*(4), 317-325.

[13]. Monroe, W. T., McQuain, M. M., Chang, M. S., Alexander, J. S., & Haselton, F. R. (1999). Targeting expression with light using caged DNA. Journal of Biological Chemistry, 274(30), 20895-20900.

[14]. Walker, J. W., McCray, J. A., & Hess, G. P. (1986). Photolabile protecting groups for an acetylcholine receptor ligand. Synthesis and photochemistry of a new class of o-nitrobenzyl derivatives and their effects on receptor function. Biochemistry, 25(7), 1799-1805.

[15]. Milburn, T., Matsubara, N., Billington, A. P., Udgaonkar, J. B., Walker, J. W., Carpenter, B. K., ... & Denk, W. (1989). Synthesis, photochemistry, and biological activity of a caged photolabile acetylcholine receptor ligand. Biochemistry, 28(1), 49-55.

[16]. Wieboldt, R., Gee, K. R., Niu, L., Ramesh, D., Carpenter, B. K., & Hess, G. P. (1994). Photolabile precursors of glutamate: synthesis, photochemical properties, and activation of glutamate receptors on a microsecond time scale. Proceedings of the National Academy of Sciences, 91(19), 8752-8756.

[17]. Matsuzaki, M., Ellis-Davies, G. C., Nemoto, T., Miyashita, Y., Iino, M., & Kasai, H. (2001). Dendritic spine geometry is critical for AMPA receptor expression in hippocampal CA1 pyramidal neurons. Nature neuroscience, 4(11), 1086-1092.

[18]. Breitinger, H. G. A., Wieboldt, R., Ramesh, D., Carpenter, B. K., & Hess, G. P. (2000). Synthesis and characterization of photolabile derivatives of serotonin for chemical kinetic investigations of the serotonin 5-HT3 receptor. Biochemistry, 39(18), 5500-5508.

[19]. Breitinger, H. G. A., Wieboldt, R., Ramesh, D., Carpenter, B. K., & Hess, G. P. (2000). Synthesis and characterization of photolabile derivatives of serotonin for chemical kinetic investigations of the serotonin 5-HT3 receptor. Biochemistry, 39(18), 5500-5508.

[20]. Banerjee, A., Grewer, C., Ramakrishnan, L., Jäger, J., Gameiro, A., Breitinger, H. G. A., ... & Hess, G. P. (2003). Toward the development of new photolabile protecting groups that can rapidly release bioactive compounds upon photolysis with visible light. The Journal of organic chemistry, 68(22), 8361-8367.

[21]. Shembekar, V. R., Chen, Y., Carpenter, B. K., & Hess, G. P. (2005). A protecting group for carboxylic acids that can be photolyzed by visible light. Biochemistry, 44(19), 7107-7114.

[22]. Shembekar, V. R., Chen, Y., Carpenter, B. K., & Hess, G. P. (2007). Coumarin-caged glycine that can be photolyzed within 3 μs by visible light. Biochemistry, 46(18), 5479-5484.

[23]. Ellis-Davies, G. C. (2013). A chemist and biologist talk to each other about caged neurotransmitters. Beilstein journal of organic chemistry, 9(1), 64-73.

[24]. Fino, E., Araya, R., Peterka, D. S., Salierno, M., Etchenique, R., & Yuste, R. (2009). RuBi-glutamate: two-photon and visible-light photoactivation of neurons and dendritic spines. Frontiers in neural circuits, 3, 2.

[25]. McMillan, T. J., Leatherman, E., Ridley, A., Shorrocks, J., Tobi, S. E., & Whiteside, J. R. (2008). Cellular effects of long wavelength UV light (UVA) in mammalian cells. Journal of Pharmacy and Pharmacology, 60(8), 969-976.

[26]. Callaway, E. M., & Yuste, R. (2002). Stimulating neurons with light. Current opinion in neurobiology, 12(5), 587-592.

[27]. Dalva, M. B., & Katz, L. C. (1994). Rearrangements of synaptic connections in visual cortex revealed by laser photostimulation. SCIENCE-NEW YORK THEN WASHINGTON-, 255-255.

[28]. Dodt, H. U., Frick, A., Kampe, K., & Zieglgänsberger, W. (1998). NMDA and AMPA receptors on neocortical neurons are differentially distributed. European journal of Neuroscience, 10(11), 3351-3357.

[29]. Frick, A., Zieglgänsberger, W., & Dodt, H. U. (2001). Glutamate receptors form hot spots on apical dendrites of neocortical pyramidal neurons. Journal of neurophysiology, 86(3), 1412-1421.

[30]. Schiller, J., Schiller, Y., & Clapham, D. E. (1998). NMDA receptors amplify calcium influx into dendritic spines during associative pre-and postsynaptic activation. *Nature neuroscience*, *1*(2), 114-118.

[31]. Wang, S. S. H., Khiroug, L., & Augustine, G. J. (2000). Quantification of spread of cerebellar long-term depression with chemical two-photon uncaging of glutamate. *Proceedings of the National Academy of Sciences*, *97*(15), 8635-8640.

[32]. Sobczyk, A., Scheuss, V., & Svoboda, K. (2005). NMDA receptor subunit-dependent [Ca2+] signaling in individual hippocampal dendritic spines. The Journal of neuroscience, 25(26), 6037-6046.

[33]. Yang, S. N., Tang, Y. G., & Zucker, R. S. (1999). Selective induction of LTP and LTD by postsynaptic [Ca2+] i elevation. Journal of neurophysiology, 81(2), 781-787.

[34]. Nikolenko, V., Watson, B. O., Araya, R., Woodruff, A., Peterka, D. S., & Yuste, R. (2008). SLM Microscopy: scanless two-photon imaging and photostimulation using spatial light modulators. Frontiers in neural circuits, 2, 5.

[35]. Lutz, C., Otis, T. S., DeSars, V., Charpak, S., DiGregorio, D. A., & Emiliani, V. (2008). Holographic photolysis of caged neurotransmitters. Nature Methods, 5(9), 821-827.

[36]. Zahid, M., Vélez-Fort, M., Papagiakoumou, E., Ventalon, C., Angulo, M. C., & Emiliani, V. (2010). Holographic photolysis for multiple cell stimulation in mouse hippocampal slices. PLoS One, 5(2), e9431.

[37]. Dal Maschio, M., Difato, F., Beltramo, R., Blau, A., Benfenati, F., & Fellin, T. (2010). Simultaneous two-photon imaging and photo-stimulation with structured light illumination. Optics express, 18(18), 18720-18731.

[38]. Papagiakoumou, E., Anselmi, F., Bègue, A., de Sars, V., Glückstad, J., Isacoff, E. Y., & Emiliani, V. (2010). Scanless two-photon excitation of channelrhodopsin-2. Nature methods, 7(10), 848-854.

[39]. Anselmi, F., Ventalon, C., Bègue, A., Ogden, D., & Emiliani, V. (2011). Three-dimensional imaging and photostimulation by remote-focusing and holographic light patterning. Proceedings of the National Academy of Sciences, 108(49), 19504-19509.

[40]. Yang, S., Papagiakoumou, E., Guillon, M., de Sars, V., Tang, C. M., & Emiliani, V. (2011). Three-dimensional holographic photostimulation of the dendritic arbor. Journal of neural engineering, 8(4), 046002.

[41]. Go, M. A., To, M. S., Stricker, C., Redman, S., Bachor, H. A., Stuart, G. J., & Daria, V. R. (2013). Four-dimensional multi-site photolysis of caged neurotransmitters. Frontiers in cellular neuroscience, 7.

[42]. Godwin, D. W., Che, D., O'Malley, D. M., & Zhou, Q. (1997). Photostimulation with caged neurotransmitters using fiber optic lightguides. *Journal of neuroscience methods*, *73*(1), 91-106.

[43]. Parpura, V., & Haydon, P. G. (1999). UV photolysis using a micromanipulated optical fiber to deliver UV energy directly to the sample. *Journal of neuroscience methods*, *87*(1), 25-34.

[44]. Ghezzi, D., Menegon, A., Pedrocchi, A., Valtorta, F., & Ferrigno, G. (2008). A micro-electrode array device coupled to a laser-based system for the local stimulation of neurons by optical release of glutamate. *Journal of neuroscience methods*, *175*(1), 70-78.

[45]. Kandler, K., Katz, L. C., & Kauer, J. A. (1998). Focal photolysis of caged glutamate produces long-term depression of hippocampal glutamate receptors. Nature neuroscience, 1(2), 119-123.

[46]. Dong, X. X., Wang, Y., & Qin, Z. H. (2009). Molecular mechanisms of excitotoxicity and their relevance to pathogenesis of neurodegenerative diseases. Acta Pharmacologica Sinica, 30(4), 379-387

[47]. Vázquez, M. E., Nitz, M., Stehn, J., Yaffe, M. B., & Imperiali, B. (2003). Fluorescent caged phosphoserine peptides as probes to investigate phosphorylation-dependent protein associations. Journal of the American Chemical Society, 125(34), 10150-10151.

[48]. Gillis, K. D., Mößner, R., & Neher, E. (1996). Protein kinase C enhances exocytosis from chromaffin cells by increasing the size of the readily releasable pool of secretory granules. Neuron, 16(6), 1209-1220.

[49]. Heidelberger, R., Heinemann, C., Neher, E., & Matthews, G. (1994). Calcium dependence of the rate of exocytosis in a synaptic terminal.

[50]. Ellis-Davies, G. C. (2007). Caged compounds: photorelease technology for control of cellular chemistry and physiology. Nature methods, 4(8), 619-628.

[51]. Marvin, J. S., Borghuis, B. G., Tian, L., Cichon, J., Harnett, M. T., Akerboom, J., & Orger, M. B. (2013). An optimized fluorescent probe for visualizing glutamate neurotransmission. Nature methods, 10(2), 162-170.

[52]. Altevogt, B. M., Davis, M., & Pankevich, D. E. (Eds.). (2011). Glutamate-related biomarkers in drug development for disorders of the nervous system: Workshop summary. National Academies Press.

[53]. Vander's Human Physiology: The Mechanisms of Body Function 12th Edition

[54]. Specht, A., Bolze, F., Nicoud, J. F., & Goeldner, M. (2013). Characterization of one-and two-photon photochemical uncaging efficiency. Chemical Neurobiology: Methods and Protocols, 79-87.

[55]. Jang, J. M., Lee, J., Kim, H., Jeon, N. L., & Jung, W. (2016). One-photon and two-photon stimulation of neurons in a microfluidic culture system. Lab on a Chip, 16(9), 1684-1690.

[56]. Müller, J., Ballini, M., Livi, P., Chen, Y., Radivojevic, M., Shadmani, A., & Stettler, A. (2015). High-resolution CMOS MEA platform to study neurons at subcellular, cellular, and network levels. Lab on a Chip, 15(13), 2767-2780.

[57]. Lewicki, M. S. (1998). A review of methods for spike sorting: the detection and classification of neural action potentials. Network: Computation in Neural Systems, 9(4), R53-R78.

[58]. Quiroga, R. Q., Nadasdy, Z., & Ben-Shaul, Y. (2004). Unsupervised spike detection and sorting with wavelets and superparamagnetic clustering. Neural computation, 16(8), 1661-1687.

[59]. Levakova, M., Tamborrino, M., Ditlevsen, S., & Lansky, P. (2015). A review of the methods for neuronal response latency estimation. Biosystems, 136, 23-34.

[60]. Gold, C., Henze, D. A., Koch, C., & Buzsáki, G. (2006). On the origin of the extracellular action potential waveform: a modeling study. Journal of neurophysiology, 95(5), 3113-3128.

[61]. Rohatgi-Mukherjee, K. K. (1978). Fundamentals of photochemistry. New Age International.

[62]. Emerson, R. (1958). The quantum yield of photosynthesis. Annual Review of Plant Physiology, 9(1), 1-24.

[63]. Hecht, E. (2002). Optics, 4th. International edition, Addison-Wesley, San Francisco, 3.

[64]. Trigo, F. F., Corrie, J. E., & Ogden, D. (2009). Laser photolysis of caged compounds at 405nm: photochemical advantages, localisation, phototoxicity and methods for calibration. Journal of neuroscience methods, 180(1), 9-21.